Applied Geochemistry 198 (2026) 106685

Contents lists available at ScienceDirect

Applied Geochemistry

journal homepage: www.elsevier.com/locate/apgeochem

Contribution of dissolved organic carbon to total alkalinity in Enhanced Weathering experiments

Lukas Rieder [a,*], Mathilde Hagens [b], Reinaldy Poetra [a], Alix Vidal [c], Tullia Calogiuri [b,c], Anna Neubeck [d], Abhijeet Singh [d,k,l], Thomas Corbett [d], Harun Niron [e], Sara Vicca [e,f], Siegfried E. Vlaeminck [e], Iris Janssens [g], Tim Verdonck [h], Ivan Janssens [f,i], Xuming Li [a], Jens S. Hammes [j], Jens Hartmann [a]

[a] Department of Earth System Sciences, University of Hamburg, Hamburg, Germany
[b] Soil Chemistry Group, Wageningen University & Research, Wageningen, the Netherlands
[c] Soil Biology Group, Wageningen University & Research, Wageningen, the Netherlands
[d] Department of Earth Sciences, Uppsala University, Uppsala, Sweden
[e] Biobased Sustainability Engineering (SUSTAIN), University of Antwerp, Antwerpen, Belgium
[f] Global Change Ecology Centre of Excellence, University of Antwerp, Antwerpen, Belgium
[g] University of Antwerp - imec - IDLab, Department of Computer Science, 2000, Antwerpen, Belgium
[h] University of Antwerp - imec - IDLab, Department of Mathematics, 2000, Antwerpen, Belgium
[i] Department of Biology, University of Antwerp, Wilrijk, Belgium
[j] Carbon Drawdown Initiative Carbdown GmbH, Fürth, Germany
[k] Faculty of Agriculture, Allied Sciences and Technology, Ganpat University, Gujarat, India
[l] Department of Molecular Sciences, Swedish University of Agricultural Sciences, 750 07, Uppsala Sweden

ARTICLE INFO

Editorial handling by: Elisa Sacchi

Keywords:
Non-carbonate alkalinity
Carbon dioxide removal
MRV
Organic alkalinity
Organic acids
Microcosm experiments

ABSTRACT

Total Alkalinity (TA) is widely used as a proxy for captured CO_2 in enhanced weathering (EW) applications. However, organic anions can also contribute to TA. To improve carbon accounting in EW, which is often simplified to that TA equals carbonate alkalinity, their contribution should be taken into account.

In this study, we tested how dissolved organic carbon (DOC) contributes to non-carbonate alkalinity (A_{NC}) using microcosm experiments with artificial organo-mineral mixtures. We used different combinations of rock powder with straw, microbes and earthworm additions, under ambient air conditions. The microcosms were flow-through columns placed in a climate chamber at 25 °C, which were irrigated with groundwater at rates between 1200 and 3600 mm/yr. The concentrations of several low-molecular-weight organic acids (oxalate, citrate, acetate, gluconate) were quantified to assess which conjugate base anions impact the measured TA.

Results revealed a ratio of 3.5 mol DOC per A_{NC} equivalent. In the overall experiment the median contribution of A_{NC} to TA was around 5.5 %. A positive correlation between DOC and charge-balance error suggests that some organic acid anions remained deprotonated during TA titration. Acetate anions found in DOC-rich water samples further support a substantial contribution of organic anions to TA. To investigate the relevance of A_{NC} for natural EW systems, we also quantified A_{NC} contributions in natural waters and leachates from soil EW experiment mesocosms. Because DOC levels were lower, A_{NC} contributions were smaller, ranging from a median of 4.1 % in soil mesocosm leachates down to 0.9 % in Elbe estuary water samples. This A_{NC} contribution, despite seeming small, is relevant for carbon accounting in terrestrial EW practices, where TA is often assumed to be solely carbonate alkalinity.

1. Introduction

Climate change is one of the most urgent environmental problems of the 21st century. To limit anthropogenic global warming to 2 °C or lower by 2100, all IPCC emission scenarios require not only substantial emission reductions but also the deployment of carbon dioxide removal

* Corresponding author. Department of Earth System Sciences, University of Hamburg, Bundesstraße 55, 20146, Hamburg, Germany.
E-mail addresses: lukas.rieder.climate@gmail.com (L. Rieder), geo@hattes.de (J. Hartmann).

https://doi.org/10.1016/j.apgeochem.2026.106685
Received 13 June 2025; Received in revised form 1 December 2025; Accepted 6 January 2026
Available online 20 January 2026

(CDR) approaches (IPCC, 2022a, 2022b; Smith et al., 2024). One CDR approach receiving growing scientific and practical interest is enhanced weathering (EW), a novel, nature-based CDR method.

EW aims to accelerate the dissolution of rock and increase alkalinity fluxes to the oceans (Beerling et al., 2020; Goll et al., 2021; Hartmann et al., 2013; Schuiling and Krijgsman, 2006; Seifritz, 1990). Dissolution of silicate minerals is a natural process that has regulated the global carbon cycle on geological timescales, while the weathering of carbonates provides a CO_2 sink on shorter time scales due to carbonate formation in the ocean and following CO_2 degassing (Berner, 2003; Walker et al., 1981).

Due to their global abundance and rapid weathering rates, mafic and ultramafic silicate rocks are the main focus of EW application studies (Hartmann et al., 2013). Mafic and ultramafic rocks are mainly composed of low-silica silicate minerals, including olivine, pyroxene, and plagioclase. Mineral dissolution rates vary between minerals by several orders of magnitude for constant environmental conditions (Lasaga et al., 1994). Compared to terrestrial carbonate weathering, silicate weathering and transfer of bound CO_2 in the form of alkalinity into the ocean are assumed to represent a longer removal pattern. When dissolved carbonate species (HCO_3^-, CO_3^{2-}) reprecipitate as carbonate minerals (in the ocean or in soils) CO_2 is released (see Eq. (2) to Eq. (3)). As an illustrative example, the weathering reactions of wollastonite ($CaSiO_3$) and calcite ($CaCO_3$) with carbonic acid are shown below (see Eq. (1) and Eq. (2)).

Silicate dissolution	$CaSiO_{3(s)} + 2\,CO_{2(g)} + 3\,H_2O \rightarrow \mathbf{Ca^{2+}} + \mathbf{2\,HCO_3^-} + \mathbf{H_4SiO_{4(aq)}}$	Eq. 1
Carbonate dissolution	$CaCO_{3(s)} + CO_{2(g)} + H_2O \rightarrow \mathbf{Ca^{2+}} + \mathbf{2\,HCO_3^-}$	**Eq. 2**
Mineral carbonation	$\mathbf{Ca^{2+}} + \mathbf{2\,HCO_3^-} \rightarrow CaCO_{3(s)} + CO_{2(g)} + H_2O$	**Eq. 3**

After the dissolution reaction, the previously gaseous CO_2 is bound as aqueous carbonate species (HCO_3^-, CO_3^{2-}), which at a pH of around 7–8 are mostly HCO_3^- ions.

The carbonate species act as buffers to added acid in the water. To measure this buffering capacity, also called the total/titrated alkalinity (TA), water is titrated with a strong acid to a given endpoint based on the carbonate system, typically around pH = 4.3. If, in addition to the carbonate alkalinity, other species such as organic molecules add to TA, these molecules counterbalance released cations from the dissolution reaction (Eq. (1) and Eq. (2)), and reduce the captured CO_2 in the form of DIC.

The importance of the contribution of organic molecules to TA (organic alkalinity) was studied for natural freshwaters by (Liu et al., 2020; Lozovik, 2005) and in estuarine and coastal waters by (Cai et al., 1998; Hu, 2020; Kerr et al., 2021; Muller and Bleie, 2008; Song et al., 2020). Also, it was closely studied in the Baltic Sea (Hammer et al., 2017; Kuliński et al., 2014) and for seawater (Kim and Lee, 2009; Ko et al., 2016; Lee et al., 2024; Lukawska-Matuszewska, 2016; Lukawska-Matuszewska et al., 2018; Sharp and Byrne, 2020). A comprehensive review on ocean alkalinity emphasizes the distinction between titration and charge balance alkalinity (Middelburg et al., 2020).

To generate organic alkalinity, an organic acid needs to react with an alkaline substance so that the conjugate base of the organic acid is left in the solution. An example of mineral dissolution for wollastonite with an organic acid would be:

$$CaSiO_{3(s)} + 2\,R\text{–}COOH + H_2O \rightarrow \mathbf{Ca^{2+}} + \mathbf{2\,R\text{–}COO^-} + \mathbf{H_4SiO_{4(aq)}} \quad \text{Eq. 4}$$

Organic acids in natural waters originate from microbial organic matter decomposition and direct exudation by living organisms such as plants, algae, and microbes. They are weak acids and donate H^+ to the water, lowering pH. Deprotonation of functional groups on organic acids typically happens in the pH range of 3–10, depending on the overall chemical composition and structure of the respective organic acid (Pittman and Lewan, 1994).

Organic acids affect mineral dissolution rates through several processes. First, they can lower the pH of the solution and thereby impact mineral dissolution (Drever and Stillings, 1997). Second, the deprotonated organic acid conjugate base anions can form complexes with cations in the solution, also known as chelation (Pittman and Lewan, 1994). This chelation reaction can further enhance mineral dissolution rates in addition to the effect of pH alone (Welch et al., 2002; Welch and Ullman, 1993). Furthermore, the conjugate base anions can also act on the mineral surfaces and form surface complexes (Adeleke et al., 2017; Pittman and Lewan, 1994). Organic acids also have indirect effects on mineral dissolution through microorganisms, serving as a food source for them. In turn, these microorganisms release microbial metabolic byproducts that can then contribute to mineral dissolution (de los Ríos and Souza-Egipsy, 2021; Wiesenbauer et al., 2025).

A specific environmentally relevant subgroup of organic acids comprises low-molecular-weight organic acids (LMWOAs). They are widespread on the earth's surface, play central roles in the Krebs cycle (Xiao and Wu, 2014), and occur widely in soils (Tani et al., 2001). LMWOAs are also generated during the early stages of plant litter decomposition, making them common constituents of fresh litter leachates (Küsel and Drake, 1998; Lv et al., 2023). LMWOAs typically are composed of 1–6 carbon atoms and 1–3 carboxylic functional groups (Xiao and Wu, 2014). Due to their high density of ionizable functional groups relative to their molecular size, they are more water-soluble than high-molecular-weight organic acids (Perminova et al., 2003), which makes them particularly relevant for studies of natural water chemistry.

In order to quantify the contribution of dissolved organic carbon (DOC) to released TA, reducing the potential to transfer CO_2 into carbonate alkalinity, a flow-through microcosm experiment with an artificial organo-mineral mixture was set up. In addition, the concentrations of LMWOAs were measured, and their contribution to TA was discussed. To verify the validity in non-artificial systems, we compare our results with data from other EW soil column experiments and natural water samples from estuaries. This helps to define typical DOC-to-non-carbonate alkalinity ratios and the large-scale impact of DOC on TA. Understanding the importance of DOC in this context has important implications for estimating the realized CDR potential of rock weathering and contributes to knowledge of monitoring, reporting, and verification (MRV) efforts for EW-based CDR.

2. Methods

2.1. Experimental setup

The experimental setup was designed to investigate the impact of diverse biological, chemical, and physical factors on mineral dissolution by utilizing microcosms filled with artificial organo-mineral mixtures that included various soil biota under ambient conditions. By putting together the various ingredients of natural soils in different combinations, the goal was to enhance mineral dissolution rates and TA through the interactions of different organic and inorganic components. The setup included various silicate-rich rock types and organic matter types (Section 2.2) alongside a diverse array of bacteria, fungi, and earthworms (Section 2.3) to mimic the complex interactions found in natural soil environments.

The microcosms were placed in a climate chamber at a constant temperature of 25 °C. They were watered daily with natural groundwater (Table 1) from the top with automated sprinklers. The added water could flow through the microcosm/column and drain at the bottom, where it was collected and stored in a fridge below the microcosms. Experiments lasted for 56 days, during which the irrigation rates were adjusted to be between 50 and 150 mL per day. These rates correspond to 1200–3600 mm/year of precipitation, comparable to rainfall in tropical regions. After 56 days, leachate samples were taken to analyze the dissolved compounds. This experiment was a subset of a bigger

Table 1
Composition of the natural groundwater used for irrigation of the microcosms (mean ± s.d., n = 10). The values below the detection limit (bdl) have the detection limit in brackets.

Parameter	unit	Mean ± standard dev
pH		7.99 ± 0.10
Water Temperature	**°C**	14.87 ± 1.56
Electrical Conductivity (normalized to 25 °C)	**µS/cm**	194.30 ± 6.60
Measured total alkalinity (TA)	**µeq/kgw**	1551.01 ± 65.32
Total Carbon	**µmol/L**	1460.11 ± 0.08
Dissolved inorganic carbon (DIC)		1409.54 ± 8.03
Dissolved organic carbon (DOC)		44.69 ± 6.57
dissolved silica		220.58 ± 9.08
Ca^{2+}		714.72 ± 14.6
K^{+}		23.59 ± 9.02
Mg^{2+}		105.42 ± 17.68
P (total P)		0.29 ± 0.25
Na^{+}		283.22 ± 11.60
F^{-}		6.19 ± 3.38
Cl^{-}		237.89 ± 23.65
NO_2^{-}		bdl (0.01)
SO_4^{2-}		98.09 ± 11.32
PO_4^{3-}		bdl (0.01)
Br^{-}		bdl (0.005)
Charge balance error (CBE) (see Eq. (9))	**%**	−1.09 ± 0.79

experiment comprising 203 columns in the microcosm system. Overall, the experiment included 4 rounds of filling the 203 columns. The bigger experiment also used extremely alkaline steel slag, which was excluded from this analysis as it impacted the TA not with carbonates but hydroxides. Excluding those steel slag combinations, as well as those where required data were missing and thus prevented calculations, led to a subset of 383 microcosm combinations that were used for this study, allowing for a comprehensive analysis of the role of organic acids in mineral dissolution.

This study focuses on the dissolved compounds in the leachate water of the microcosms. TA, DIC, pH, and temperature are used to calculate non-carbonate alkalinity, which is then compared to the DOC. Anions and cations were also measured to calculate the charge balance error (CBE) of the leachate water samples and compare it with DOC.

Two different approaches were used to understand the contribution of organic acids to mineral dissolution. The first comparison was between the modeled carbonate alkalinity and the measured total alkalinity (Section 2.5.1). The second test determined whether the DOC affects the CBE of the water (Section 2.5.2). The analyzed dataset comprised a total of n = 383 leachate water samples (Section 2.5.1); however, not all measurements were taken for each water sample. This resulted in smaller subsets of samples for the performed CBE analysis, with n = 135 (Section 2.5.2).

2.2. Materials

The microcosm system is explained in detail in (Calogiuri et al., 2023). The columns were made from PVC tubes cut into 15 cm pieces with a double filter mesh at the bottom (Fig. 1) and are filled with organo-mineral substrates. Each column received 400 g of rock powder as the primary component of the organo-mineral mix. Additionally, 10 g of organic matter as feedstock for the biota was added to each column.

The experimental design aimed to enhance the dissolution of the rock powder by adding organic matter, microorganisms, and earthworms. To this aim, four different rock types were selected: two volcanic rocks with different compositions, dunite, and diabase (compositions see Table 2).

The two volcanic rocks, mined in the Eifel region, Germany, were obtained from *RPBL Basalt & Lava aus der Eifel*. The supplier refers to

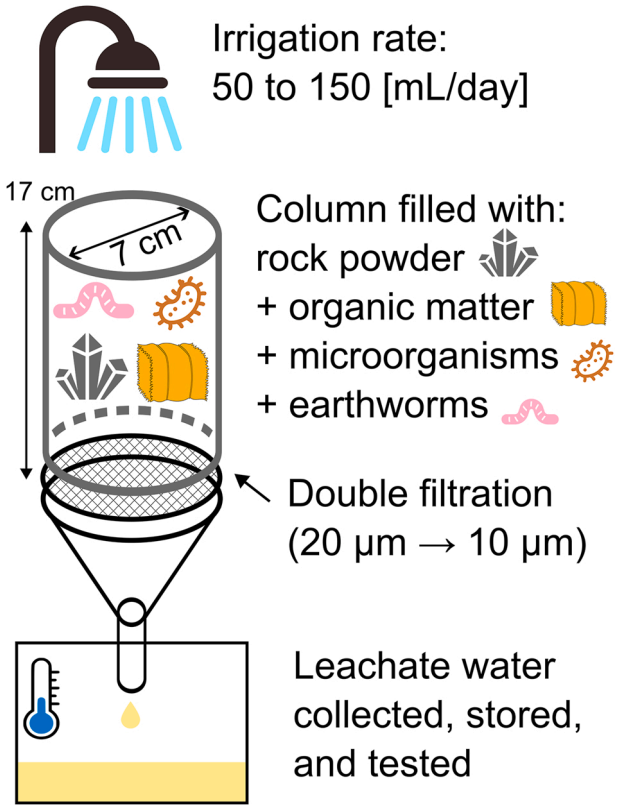

Fig. 1. Sketch of the flow-through microcosm.

Table 2
Elemental composition of the rock types was measured using X-ray fluorescence (XRF) measurements. (nd = below detection limit, LOI = loss of ignition, i.e., heating the sample to 1000 °C to gas out all carbon).

Elements	Dunite	Basalt	Basanite/Tephrite	Diabase
	mass percent (%)	mass percent (%)	mass percent (%)	mass percent (%)
SiO_2	41.55 ± 0.23	43.87 ± 0.55	43.44 ± 0.27	35.93 ± 0.73
TiO_2	0.02 ± 0.01	2.15 ± 0.06	2.58 ± 0.33	2.77 ± 0.09
Al_2O_3	0.78 ± 0.01	12.13 ± 0.18	13.79 ± 0.25	11.83 ± 0.13
Fe_2O_3	7.26 ± 0	11.66 ± 0.18	11.19 ± 0.26	13.31 ± 0.13
MnO	0.09 ± 0	0.17 ± 0	0.17 ± 0.01	0.14 ± 0.01
MgO	47.87 ± 0.24	11.4 ± 0.31	8.68 ± 0.12	4.86 ± 0.12
CaO	0.35 ± 0.19	10.41 ± 0.02	12.6 ± 0.1	14.29 ± 0.2
Na_2O	0.03 ± 0	2.26 ± 0.01	2.99 ± 0.08	1.81 ± 0.03
K_2O	0.03 ± 0.01	1.01 ± 0.06	3.29 ± 0.09	1.61 ± 0.11
P_2O_5	0.01 ± 0	0.62 ± 0	0.53 ± 0.07	0.41 ± 0.01
SO_3	nd ± nd	0.01 ± 1	0.03 ± 0.01	0.29 ± 0.18
LOI	1.8 ± 0.13	4.2 ± 2	0.62 ± 0.08	13.06 ± 1.1
Sum	99.78 ± 0.12	99.91 ± 0.07	99.91 ± 0.44	100.31 ± 0.23

them as *Basaltgestein* and *Lavagestein*, respectively. *Basaltgestein* is a dense, grey variant, while *Lavagestein* is porous and reddish-brown. According to the TAS classification, they are defined as Basalt and Basanite/Tephrite (see Supplementary Figs. 11 and 12). In the following text, they are referred to as Basalt (*Basaltgestein*) and Basanite/Tephrite (*Lavagestein*), respectively. The dunite (about 90 % olivine) was mined in Åheim, Norway, and supplied by Sibelco. The carbonate-rich, light grey diabase rock powder was sourced from Schicker Mineral, Germany. Its high $CaCO_3$ content is unusual, as this rock type typically contains little to no carbonate. This suggests that it has undergone natural

alteration through interaction with CO_2 and water, leading to the formation of carbonates. The initial elemental composition of all rock powders was measured with X-ray fluorescence (XRF; Panalytical Magix Pro; Table 2). For more details on the method, see (Calogiuri et al., 2024). To serve as a blank material, quartz sand was included, obtained from Stonewish Sand, Netherlands.

In addition to the rock materials, the study included organic amendments to feed the microorganisms and earthworms inside the microcosms. A co-digestate, a novel solid fraction of pig manure with low phosphorus content, was selected for its potential as a soil improver. This biobased fertilizer, derived from a biogas power plant, was sourced from *Groene Mineralen Centrale*, Netherlands. Finally, wheat straw, commonly used as bedding material for pets, was obtained from Pets Place, Netherlands. The elemental composition of the wheat straw and co-digestate was analyzed with ICP-MS after digestion with nitric and hydrochloric acid and heating in a microwave, adapted from the method described by Novozamsky et al. (1996). Their total carbon (C) and nitrogen (N) levels were measured using an elemental analyzer (FlashSmart, Thermo Fisher Scientific, USA). The elemental composition is shown in Table 3.

To enhance the applicability and scalability of the mineral dissolution experiments, locally sourced groundwater was used to water the microcosms. The water was pumped from a borewell on the Wageningen University campus and underwent only a single filtration step without further treatment. The composition of the input irrigation water can be found in Table 1.

2.3. Microorganisms and earthworm types

The bacteria and fungi used in this study were selected for their known capacity to enhance mineral dissolution (see references below). We inoculated the organo-mineral mixture with a selection of fungi, including *Knufia petricola* (Breitenbach et al., 2022; Gerrits et al., 2020; Pokharel et al., 2019), *Aureobasidium pullulans* (Rensink et al., 2024; Schoeman and Dickinson, 1996) and *Suillus variegatus* (Rosenstock et al., 2019; Szubstarska et al., 2012), as well as bacteria such as *Bacillus subtilis* (Liu et al., 2021; Song et al., 2007) and *Cupriavidus metallidurans* (Bryce et al., 2016; Byloos et al., 2018). The cell densities varied between 1.5×10^9 and 4.8×10^{10} cells per column for bacteria and between 5.5×10^7 and 5.5×10^8 cells per column for fungi. This work does not aim to isolate the specific contributions of inoculated fungi and bacteria to mineral dissolution, but we rather examine the overall bulk production of organic acids, which result from multiple factors, including microbial activity.

Earthworms were also tested in some microcosms. Two endogeic earthworm species, *Aporrectodea caliginosa* [Savigny] and *Allolobophora chlorotica* [Savigny], were used in the microcosms. These earthworm species were selected for this experiment due to their high abundance in the Netherlands, where the experiment took place, and their feeding habits, which primarily involve soil particles and associated organic matter (Bouché, 1977). Their effect on mineral dissolution rates in the context of this work is explained in (Calogiuri et al., 2024). In short, these effects are physical by increasing available reactive surface area (Suzuki et al., 2003) as well as chemical by increasing decomposition and releasing CO_2 (Lubbers et al., 2013; Schwartzman, 2015), and release of organic compounds from microbes living in the earthworm gut (Georgiadis et al., 2019).

2.4. Measurements in the leachate water

All leachate water samples were filtered using 0.45 μm polyether sulfone dead-end syringe filters before measurements were taken. The pH was measured using a WTW Multimeter 3430 IDS equipped with a SenTix 940 probe to assess the equilibrium stage of the carbonate system, which is essential for calculating carbonate alkalinity (Section 2.5.1). Electrical conductivity (EC) was determined with non-linear

Table 3
Elemental composition of the organic matter used in the microcosms, presented as mean ± s.d. (n = 4).

Organic matter type	C [mg/g]	N [mg/g]	C:N ratio [g:g]	K [mg/g]	Na [mg/g]	Ca [mg/g]	Mg [mg/g]	P [mg/g]	Zn [mg/g]	Fe [mg/g]	Mn [mg/g]
Wheat straw	443.64 ± 9.83	5.16 ± 0.97	85.98 ± 16.27	8.00 ± 0.08	0.019 ± 0.002	2.92 ± 0.07	0.46 ± 0.01	0.47 ± 0.01	0.004 ± 0.001	0.112 ± 0.016	0.051 ± 0.001
Co-digestate	442.24 ± 6.90	8.76 ± 0.53	50.48 ± 3.15	2.75 ± 0.06	0.914 ± 0.012	12.38 ± 0.91	1.31 ± 0.01	4.72 ± 0.38	0.14 ± 0.006	1.176 ± 0.092	0.120 ± 0.005

temperature compensation at a reference temperature of 25 °C, following DIN EN 27888 (1993), using the same multimeter fitted with a TetraCon® 925 probe. Total alkalinity (TA) was analyzed using an automated Gran potentiometric titration with 4 pH endpoints at [4.5, 4.3, 4.0, 3.7], based on Koenig (2005). The titration was performed using a Metrohm 888 Titrando, equipped with a 10/20 mL cylinder volume and an Aquatrode plus pH electrode.

Elemental concentrations, including Ca, Mg, K, P, Fe, Ni, Cr, Sr, Cu, Al, Li, Mn, and Zn, were determined using either ICP-MS or ICP-OES, depending on concentration levels. ICP-MS measurements were conducted with a Thermo Scientific™ Element2™, while ICP-OES measurements were performed using a Thermo Scientific™ iCAP 6500 duo. Anions, including fluoride (F^-), chloride (Cl^-), nitrite (NO_2^-), nitrate (NO_3^-), and sulfate (SO_4^{2-}), were analyzed using ion chromatography with a Metrohm 881 Compact IC Pro system and a Metrosep A Supp 17–150/4.0 column. For selected samples organic anions were tested. Specifically, low-molecular-weight organic acid anions, including citrate, oxalate, acetate, and gluconate, were analyzed using a Metrohm 883 Basic IC Plus ion chromatography system with a Metrosep A Supp 5 (250 × 4.0 mm) column.

Furthermore, dissolved silica (DSi) was quantified photometrically at a wavelength of 810 nm using the molybdate-blue method, as described by Hansen and Koroleff (1999). The analysis was conducted with a Hach Lange spectrophotometer DR3800 (Type: LPG 424.99.00001). To solve the carbonate system and check the relationship of A_{NC}, the dissolved inorganic carbon (DIC) and dissolved organic carbon (DOC) were measured using a catalytic combustion-based TOC analyzer (FormacsHT TOC analyzer, Skalar, NLD). DIC detection was achieved by acidifying the sample with 4 % H_3PO_4.

2.5. Calculations

2.5.1. Modelling of the non-carbonate alkalinity contribution

To model the non-carbonate alkalinity (A_{NC}), first, the carbonate alkalinity (A_C) was calculated and then subtracted from the measured TA ($TA_{measured}$) similar to previous studies (Hammer et al., 2017; Ko et al., 2016; Kuliński et al., 2014; Song et al., 2020; Yang et al., 2015). To calculate A_C (Eq. (5)), we applied a simplified model using only the dissolved inorganic carbon (DIC), pH, and temperature (T) observed in the leachate water right after sampling. Based on this set of variables, A_C was calculated using phreeqpython (Heinsbroek, 2021), assuming a closed system (DIC = const) (see Supplementary Fig. 1).

One might correctly assume that this set of variables is insufficient and too simple to model A_C. Considering that all cations and anions impact the ionic strength (*I*) of the water sample, these should be included as well to accurately calculate A_C. With the lack of including all ions in the A_C model, the *I* will be underestimated (Solomon, 2001). When the ionic strength of the aqueous solution is underestimated, the stoichiometric first and second dissociation constants of carbonic acid are overestimated (Harned and Davis Jr, 1943; Hastings and Sendroy Jr, 1925; Wolf-Gladrow et al., 2007). This overestimation will lead to a lower modeled A_C than the A_C modeled from the full set of ions. To check whether this simplified model is sufficient, both models are compared. For 211 water samples, it was checked how the full A_C model (cations, anions, T, pH, DIC) compares to the simple A_C model (T, pH, DIC). They do match to a sufficient extent for our analysis (see Supplementary Fig. 2). This allowed us to use all 383 samples for the calculation of A_C. In the following text the squared brackets imply the concentration of the compound is meant, i.e. $c(CO_3^{2-}) = [CO_3^{2-}]$ [mol/kgw]:

$$A_C = [HCO_3^-] + 2\cdot[CO_3^{2-}] \quad \text{Eq. 5}$$

The modeled A_C was then subtracted from the $TA_{measured}$. The difference between the two terms is A_{NC}. Any conjugate base of a (weak) acid that can accept protons until the endpoint of the modified Gran titration (see Supplementary Section 1) will contribute to the measured total alkalinity. Assuming that other inorganic compounds able to buffer will be minor contributors, $TA_{measured}$ can be described in the following way:

$$TA_{measured} = A_C + A_{org} + \text{minor} \quad \text{Eq. 6}$$

$$A_{NC} = TA_{measured} - A_C = A_{org} + \text{minor} \approx A_{org} \quad \text{Eq. 7}$$

In addition, we also calculate the fraction of non-carbonate alkalinity as ($A_{NC}/TA_{measured}$). This is highly relevant in the context of CDR, where the non-carbonate fraction should ideally be as small as possible. Because $TA_{measured}$ is often used as a direct measure for the captured CO_2 in inorganic form, large concentrations of A_{NC} will complicate the overall assessment of CO_2 capture and shift the focus to the generation and decomposition pathways of the involved organic molecules.

2.5.2. Calculating the charge balance of the water

The charge balance error (CBE) is a quality check in aquatic geochemistry that assesses the consistency of measured cation and anion concentrations in a water sample. It is calculated as the relative difference between the total equivalent concentrations of cations and anions and is used to identify potential analytical errors, missing ions, or inconsistencies in water chemistry data. Part of the involved anions are conjugate bases of organic acids, which have a wide range of pK values (Schwarzenbach et al., 2003) and thereby impact CBE. In aquatic geochemistry anions are divided into two fractions: the conservative anions and the alkalinity contributors (Stumm and Morgan, 1996). The conservative anions are conjugate base anions from strong acids. The other anions are the conjugate base anions of weak acids to a given reference level, which is defined by the titration endpoints. The presence of a conjugate base of an organic acid with a low pK, i.e., lower than or inside the titration endpoint pH window of 4.5 to 3.7, leads to un-neutralized organic anions that are left in the water after the alkalinity titration. Thus, these conjugate base anions are missing in the $TA_{measured}$. When these are not quantified in another way and included in the calculation (Eq. (8)), it will lead to an excess of cations over anions and thus a positive CBE. For this study, this missing alkalinity is called $A_{low\text{-}pH}$.

In the case of accurate measurements, the CBE values should form a distribution with a median value of CBE = 0 % and a variance as small as possible. Any systematic positive trends show that a negative charge is missing in the determination.

$$TA_{measured} = \sum \text{cations} - \sum \text{anions} \quad \text{Eq. 8}$$

In this study with:	
Cations:	**Anions:** **Anions that do not buffer pH in the range of alkalinity titration (conservative anions)**
Na^+, K^+, Mg^{2+}, Ca^{2+}	Cl^-, F^-, NO_2^-, NO_3^-, SO_4^{2-}

Based on Eq. (8) the charge balance error (CBE) for water samples can be defined as:

$$CBE\ [\%] = \frac{\sum \text{cations} - (\sum \text{anions} + TA_{measured})}{\sum \text{cations} + (\sum \text{anions} + TA_{measured})} \cdot 100 \quad \text{Eq. 9}$$

For seawater with high ionic strength and low DOC content, this definition (Eq. (9)) usually fits well with the commonly accepted charge balance error (CBE) of below 5 % (DIN 38402-62, 2014; Fritz, 1994). However, in low ionic strength, high DOC freshwaters, such as the tested leachate water, CBEs are usually larger than 5 %. One must therefore know the organic anion concentrations and other alkalinity contributions and include them in the definition to lower the calculated CBE.

For the tested leachate water samples the hypothesis is that the organic anions can describe the missing part, therefore this simple

equation will be expanded by adding the unprotonated part ($A_{low\text{-}pH}$) that does not buffer to the given pH endpoints of the alkalinity titration:

$$TA_{measured} + A_{low-pH} = \sum \text{cations} - \sum \text{anions} \quad \text{Eq. 10}$$

Moving $TA_{measured}$ to the right-hand side we get the following definition:

$$A_{low-pH} = \Delta\text{charge} = \sum \text{cations} - \left(\sum \text{anions} + TA_{measured}\right) \quad \text{Eq. 11}$$

The CBE [%] (Eq. (9)) will be calculated and plotted against the DOC concentration for the analyzed water samples. When organic compounds are driving the charge balance error, the DOC must correlate with a positive charge balance error. Therefore, a linear regression is performed with x = CBE and y = DOC.

2.5.3. Determination of LMWOAs

Based on the large values for A_{NC} and CBE of the previous calculations, it was decided to also monitor the concentrations of certain LMWOAs. A water sample with large A_{NC} must contain more organic alkalinity and thus detectable organic acid conjugate base anions.

To determine which organic acid anions are present in the water samples, a subset of the samples ($A_{NC} \geq 3$ meq/kgw) was analyzed for acetate, oxalate, gluconate, and citrate. These samples with high A_{NC} are potentially have higher concentrations of the conjugate bases of LMWOAs compared to the samples with low A_{NC}. Table 4 shows the dissociation constants of selected acids, including the LMWOAs tested in the setup.

In case of abundant LMWOAs, their speciation was modeled with phreeqpython (Heinsbroek, 2021) using the 'minteq.v4.dat' database for the organic acid constants that were derived from (US EPAO, 2013).

3. Results and discussion

3.1. Non-carbonate alkalinity (A_{NC}) determination

First the A_C is plotted against the $TA_{measured}$ to give a first impression of non-carbonate alkalinity (Fig. 2). In the diagram we can divide the datapoints by the 1:1 line into two areas. One is the area above the 1:1 line where the calculations imply that A_C is bigger than $TA_{measured}$. This is conceptually impossible, given that A_C is a part of $TA_{measured}$. One can see very few datapoints above this line, which is also a good indication of the data quality. An A_C larger than $TA_{measured}$ usually indicates that DIC or pH has been overestimated (Dickson et al., 2007).

More interesting is the area below the 1:1 line where the $TA_{measured}$ exceeds A_C. This results in the calculated A_{NC} to be positive. The uncertainty in A_{NC} was propagated from the standard deviation of $TA_{measured}$ input water replicates and the error in A_C for each sample using standard error propagation rules. The resulting mean propagated uncertainty across all samples was 0.066 meq/kgw. Out of the 383 samples 350 had an A_{NC} bigger than the error in the A_{NC} determination.

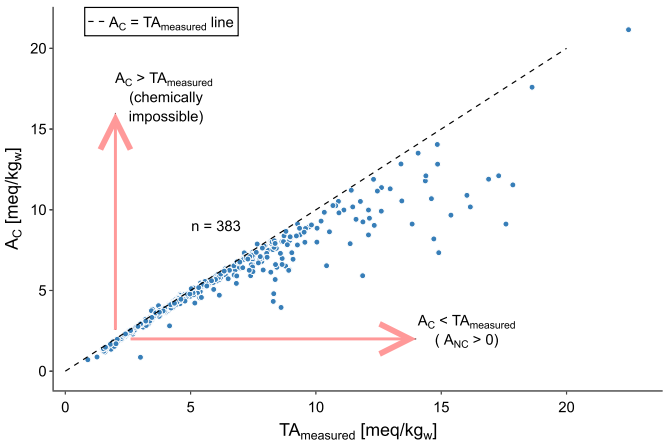

Fig. 2. Calculated carbonate alkalinity (A_C) vs. measured total alkalinity ($TA_{measured}$).

The A_{NC} varied from −0.357 meq/kgw to 8.466 meq/kgw.

In the next diagram (Fig. 3), the calculated A_{NC} is plotted against $TA_{measured}$. Most of the data points are spread close to the $A_{NC} = 0$ line. This implies that the produced alkalinity must be close to the carbonate alkalinity ($TA_{measured} \approx A_C$). From Fig. 4 it is also possible to observe, that A_{NC} also grows with $TA_{measured}$ for DOC-rich samples. As the alkalinity in the microcosm environment was increased also the release of DOC was increased due to the higher pH. This trend in DOC concentrations is also visible in the plot. Low DOC samples also show low A_{NC}.

To better understand the relationship between DOC and A_{NC}, we display the DOC concentration against A_{NC} (Fig. 4). All points as a bulk show the pattern of an increasing DOC with A_{NC}, but some small variations are visible. We observe an accumulation of datapoints with low DOC concentrations and low A_{NC} in the bottom-left corner.

From the relationship between DOC and A_{NC}, we can learn something about the nature of the organic molecules that make up the DOC. The trendline in Fig. 4 illustrates the relationship between the number of organic carbon atoms and alkalinity equivalents. Because of the theoretical proportional relationship of conjugate base anions and $TA_{measured}$ a linear relationship was used to describe the pattern and the data seem to fit this relationship.

From the ratio of DOC to A_{NC}, one can infer the characteristics of the organic molecules that have contributed to the observed alkalinity. The relationship shows how much DOC is needed to impact the alkalinity. In theory, a huge intercept and huge slope would tell us that there is a lot of uncharged DOC present with only a few deprotonation sites per organic carbon atom. A small intercept and slope would tell us there is a big charge density and more deprotonation sites per carbon atom. Two factors might drive this intercept and slope. First, the measurement uncertainty in DOC and A_{NC} will lead to variation in the regression parameters. Second, the quality of DOC, as the involved organic molecules

Table 4
Acid constants of selected organic and inorganic acids. The pK values are in most cases below the typical endpoint for Gran titration for determining TA. All shown acid constants are for T = 25 °C and I = 0 taken from NIST 46.4 (NIST46, 2013).

Compound (trivial name)	Preferred IUPAC name	Formula	pK_{a1}	pK_{a2}	pK_{a3}	ratios [carbon atoms/charge] for the different deprotonation stages
Acetic acid	Acetic acid	$C_2H_4O_2$	4.757	–	–	2
Lactic acid	2-Hydroxypropanoic acid	$C_3H_6O_3$	3.860	–	–	3
Malic acid	2-Hydroxybutanedioic acid	$C_4H_6O_5$	3.459	5.097	–	4, 2
Oxalic acid	Oxalic acid	$C_2H_2O_4$	1.250	4.266	–	2, 1
Citric acid	2-Hydroxypropane-1,2,3-tricarboxylic acid	$C_6H_8O_6$	3.128	4.761	6.396	6, 3, 2
Carbonic acid	Carbonic acid	H_2CO_3	6.325	10.329	–	1, 0.5
Gluconic acid	D-*gluco*-Pentahydroxyhexanoic acid (d-Gluconic acid)	$C_6H_{12}O_7$	3.46 (for I = 0.1)	–	–	6

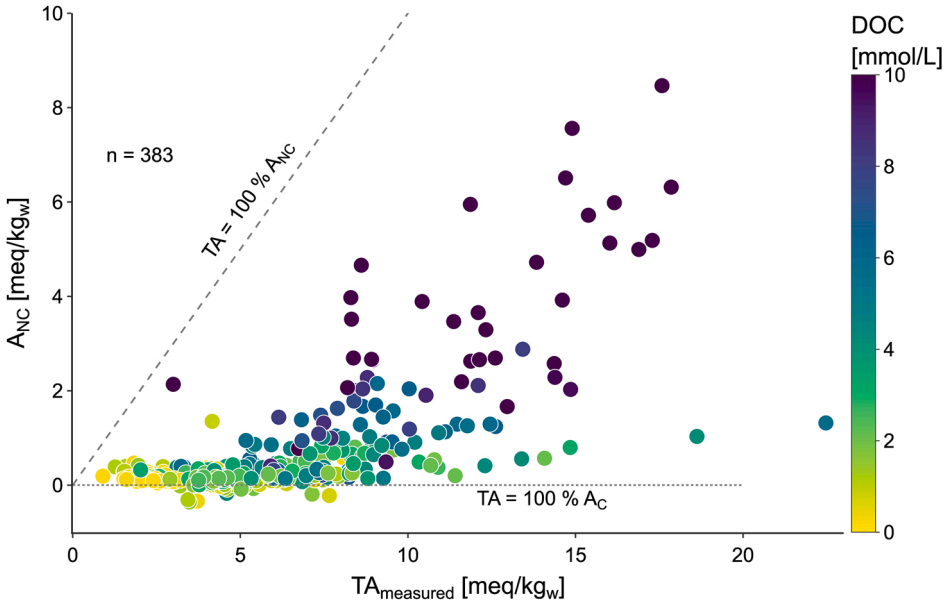

Fig. 3. Non-carbonate alkalinity (A_{NC}) versus measured alkalinity, with dissolved organic carbon (DOC) concentration represented by color. The dashed and dotted lines show the cases of pure A_{NC} and pure A_C, respectively. (For interpretation of the references to color in this figure legend, the reader is referred to the Web version of this article.)

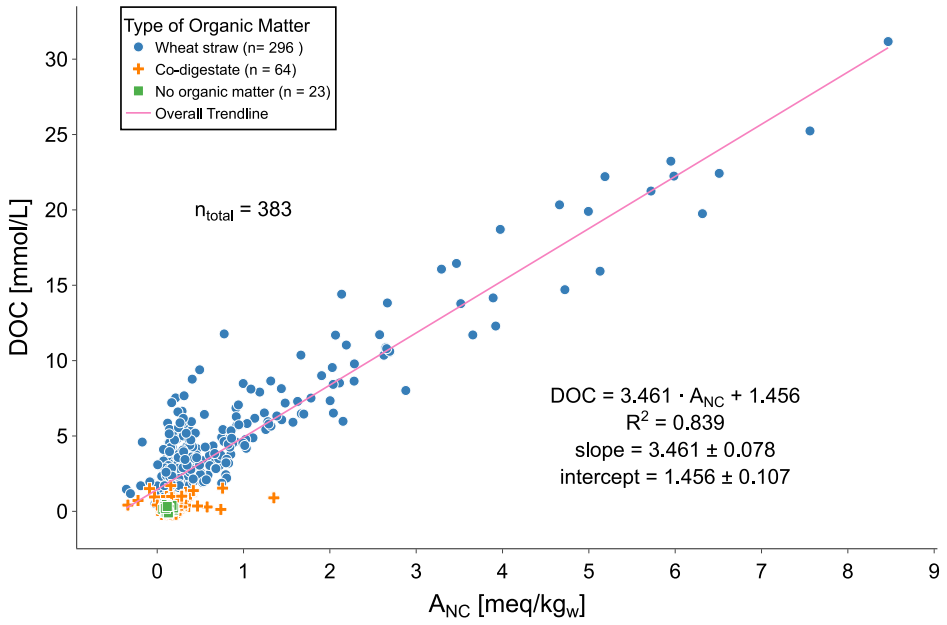

Fig. 4. Relationship between dissolved organic carbon (DOC) concentration and non-carbonate alkalinity (A_{NC}) for all selected samples (n = 383). Different organic matter sources used in the microcosms are distinguished by color. The plot includes an ordinary least squares (OLS) regression, with A_{NC} [meq/kgw] on the x-axis and DOC [mmol/L] on the y-axis. Standard errors are indicated by the ± symbol in the regression equation. (For interpretation of the references to color in this figure legend, the reader is referred to the Web version of this article.)

have a varying amount of carbon atoms and functional groups that act as deprotonation sites (Boyer et al., 2008; Mostofa et al., 2013; Vogt et al., 2024).

For the analyzed water samples, the ratio of DOC to A_{NC} is roughly 3.5, indicating that 3.5 mol of organic carbon correspond to 1 equivalent of alkalinity. This factor gives an insight into the nature of the dissolved organic molecules. LMWOAs would fulfill this criterion. Their molecules generally comprise 1–6 carbon atoms and have 1–3 carboxylic groups (Xiao and Wu, 2014), which can either donate or accept protons (see Table 4). In an alkaline solution (pH > 7) as observed in all microcosms leachate waters, the organic acids primarily consist of their deprotonated conjugate bases. Like the carbonate species, those conjugate bases will buffer acid input, contributing to the titrated alkalinity.

3.2. Charge balance error (CBE) analysis

Additionally, in the CBE-DOC diagram (Fig. 5), the impact of organic alkalinity is demonstrated. A positive CBE either indicates that the measurements of major cations and anions are inaccurate or reveals inconsistency with the TA determination. For our dataset, the latter is the case for the DOC-rich samples.

Most CBE values for leachate samples with a DOC below 5 mmol/L

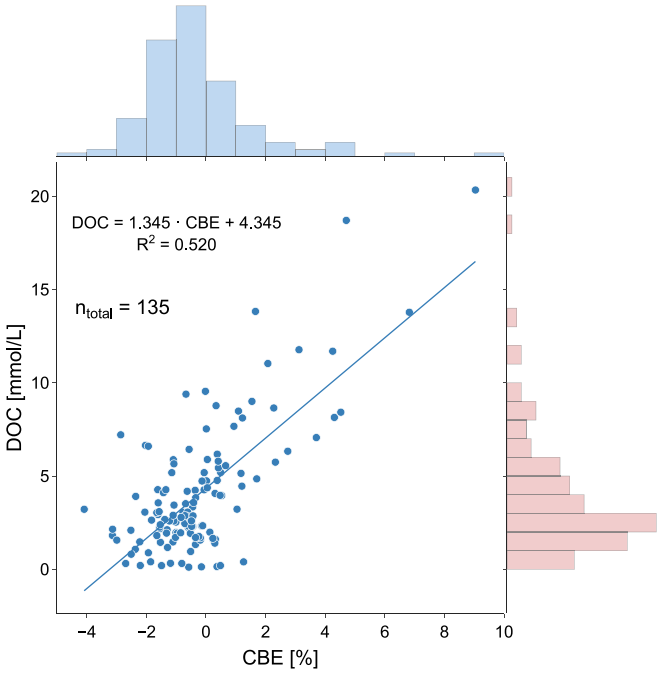

Fig. 5. DOC against the charge balance error (CBE). The CBE was calculated following Eq. (9) using $TA_{measured}$, ICP cation data and IC inorganic anions.

range from −4 to 4 % (Fig. 5). There is no clear positive trend in CBE for such low DOC samples. For leachate water samples with DOC <5 mmol/L, the overall mean CBE is −1.53 ± 4.32 %. That is why the overall distribution yields a comparably weak coefficient of determination of 0.52 (52.05 %). More leachate water samples with higher DOC concentrations would strengthen the relationship.

When examining the samples with higher DOC concentrations, the systematic relationship between the incomplete CBE and DOC becomes more visible. For samples with DOC concentrations of at least 5 mmol/L, the overall mean CBE is 1.84 ± 5.65 %. For samples with DOC concentrations of at least 10 mmol/L, the overall mean CBE is 4.37 ± 5.28 %. The standard deviation remains large due to the heterogeneous nature of the leachate water samples included.

The CBE-DOC plot demonstrates how the CBE (positively) grows with the DOC. This positive trend indicates that the unprotonated organic anions remaining in the solution represent a portion of the actual alkalinity that is not accounted for. Capturing also these missing anions can be done by selecting lower endpoints for the alkalinity titration. As A_C remains constant a lower titration endpoint will potentially increase $TA_{measured}$ and thereby A_{NC}. Then the aforementioned factor of DOC to A_{NC} of 3.5 will slightly decrease. How the titration procedure could be improved is described in Section 3.4.

3.3. Analysis of LMWOAs

To see which organic acids anions drive the A_{NC} and CBE, we selected water samples with $A_{NC} \geq 3$ meq/kgw. Due to the high A_{NC} and high DOC, these samples have the greatest potential for detecting LMWOAs. From the tested species, only acetate was found; citrate, gluconate, and oxalate were not detected in the leachate water (Fig. 6). The lack of citrate and oxalate can be explained because they are polydentate ligands, also known as chelates, while acetate is a monodentate ligand in solution (Miessler et al., 2014). Oxalate and citrate anions can form stable chelate rings together with metal cations. These can precipitate and leave the aqueous phase and form solids. Some examples are calcium oxalate monohydrate with a solubility of 0.00061 g/100 g (20 °C) (David R. Lide, 2005) also known as kidney stones, iron(II) oxalate dihydrate with solubility of 0.078 g/100 g (25 °C) (David R. Lide, 2005) known as humboldtine mineral (Müller et al., 2021) and tricalcium dicitrate tetrahydrate with solubility of 0.3081 g/100 mL (25 °C) (Vavrusova and Skibsted, 2016) also known as the earlandite mineral (Herdtweck et al., 2011). Thus, the oxalate and citrate anions might have formed complexes with metal cations and precipitated at some point in the setup or were removed by the 0.45 µm filters before analyzing the leachate water. Gluconate, in contrast, is known to form stable complexes with high solubility (Kutus et al., 2020), so it might have simply not been generated inside the microcosms.

In contrast, acetate's monodentate binding and monovalent charge result in weaker complexes that remain soluble under most conditions and are less prone to form precipitates (Van Der Sluys, 2001). However, only the acetate concentration is not enough to explain the whole A_{NC}. Also, decomposition into other organic anions or complete remineralization into CO_2 and A_C (Hu, 2020) might have occurred in the time between the measurement of main variables and the organic anion measurements. Moreover a wide variety of untested low molecular weight organic acids, each present in low concentrations, and with properties similar to acetate, such as formate and lactate (Lazo et al., 2017; Neaman, 2005), could collectively account for the observed bulk signal in A_{NC}.

For the tested DOC-rich samples, A_{NC} contributes between 30 % and 50 % of the $TA_{measured}$ (Fig. 6). Acetate was abundant in the water samples tested. Its theoretical contribution to the acid buffering capacity of water is such that 1 mol/L of acetate corresponds to 1 equivalent of alkalinity. However, when testing the $TA_{measured}$, one selects certain endpoints to calculate the TA from. For this study, an automated gran potentiometric titration with the endpoints [4.5, 4.3, 4.0, 3.7] was used to measure TA based on (Koenig, 2005). For that pH range, the acetate anions ($pK = 4.757$ see Table 4) will not be far from entirely protonated, which will lead to an underestimation of the TA (see grey lines in Fig. 7). That is why acetate in Fig. 6 is presented solely as concentration without percentage.

3.4. Improved titration for organic alkalinity

To capture the full contribution of acetate and other organic acids, it is necessary to select lower pH endpoints. For the DOC-rich samples, the actual TA will thus be larger. The actual A_{NC} will also be larger because the carbonate alkalinity (A_C) will not change as it was modeled from DIC.

A part of the organic acid conjugate base anions, for example acetate, is not measured due to the selected titration endpoints (Fig. 7). This not captured part is then missing in the $TA_{measured}$ and leads to an imbalance towards the positive CBE, because there is more total positive charge

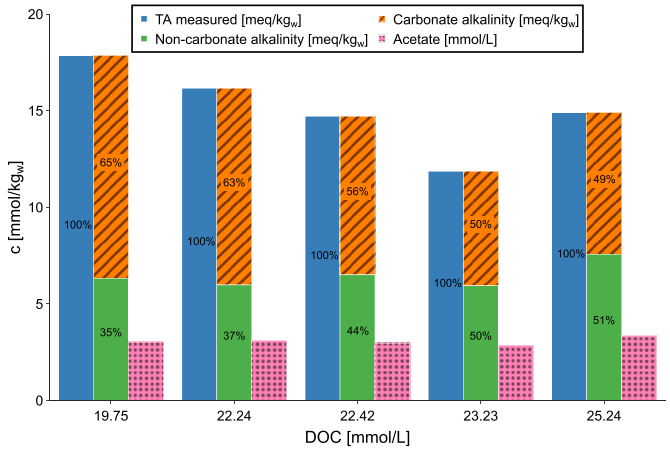

Fig. 6. Organic anions tested in the leachate water in selected DOC-rich leachate samples with $A_{NC} \geq 3$ meq/kgw. Oxalate, citrate, and gluconate were not detected in the tested leachate water.

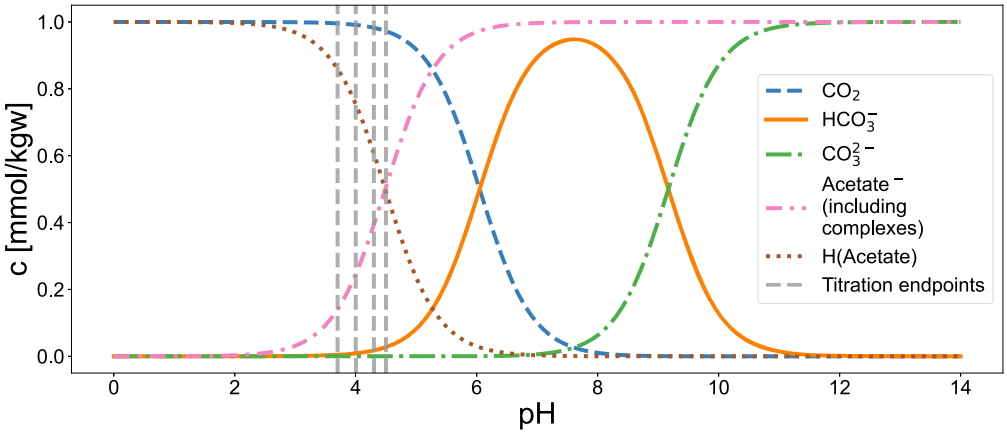

Fig. 7. Acetate (1 mmol NaAcetate) and carbonate (1 mmol $NaHCO_3$) system speciation at T = 25 °C. Modeled with phreeqpython (Heinsbroek, 2021) using the 'minteq.v4.dat' database (US EPAO, 2013) (closed system DIC = 0.001 mol/kg). NaOH is added to the solution to raise the pH, and HCl is added to lower it. The vertical lines indicate the endpoints used for the alkalinity titration [4.5; 4.3, 4.0; 3.7] after (Koenig, 2005).

than negative charge put into the calculation (see Eq. (11)). To close this gap, one needs to know what organic anions are expected in the leachate water sample to select the pH endpoints of the alkalinity titration to it. For any weak acids, the titration endpoint should be selected following the Henderson-Hasselbach equation (Po and Senozan, 2001):

$$pH = pK_{a1} + \log_{10}\left(\frac{[A^-]}{[HA]}\right). \quad \text{Eq. 12}$$

In the buffering range of the weak acid, it can be described with the degree of titration τ:

$$pH = pK_{a1} + \log_{10}\left(\frac{\tau}{1-\tau}\right). \quad \text{Eq. 13}$$

Targeting that 99 % of the weak acid should be in HA form and just 1 % of unprotonated A^- left it will lead to $\tau = 0.01$ and thus $\log_{10}(0.01/(1 - 0.01)) \approx -2$. Putting it into the equation, we get the appropriate pH endpoint that should be selected: $pH = pK_{a1} - 2$.

However, lowering the endpoint of the titration will also protonate more of the inorganic proton acceptors that need to be accounted for. In the tested water samples from the microcosms, those other inorganic species were considered negligible. In seawater, for example, this cannot be neglected for a precise assessment. The contribution of other inorganic proton acceptors is explained by Wolf-Gladrow et al. (2007).

In general, for all water sample types, to isolate the organic alkalinity, the best practice is to perform a regular titration to remove all A_C, then bubble N_2 gas the sample to strip away all CO_2 while performing the back titration with NaOH and incorporating it into the calculation as presented in multiple studies (Cai et al., 1998; Hunt et al., 2011; Kerr et al., 2021; Ko et al., 2016; Yang et al., 2015).

3.5. DOC source and dilution effect

Having discussed how the generated DOC affects the water chemistry, we can now examine the source of the DOC. For most microcosms (n = 296), wheat straw was used (see Fig. 4). Wheat straw is generally composed of 34–40 % cellulose, 20–25 % hemicellulose, and 20 % lignin (Rodriguez-Gomez et al., 2012). Those complex carbohydrates are broken down into soluble compounds and increase the DOC concentration in the leachate water. The microorganisms attached to the wheat straw begin to break it down once the straw becomes moist. The co-digestate substrate does not leach much DOC as it is already processed material from a biogas power plant, and the most labile parts of the OM have already been lost during the processing (Karki et al., 2021).

However, the presence of wheat straw alone cannot account for the huge variation in DOC concentrations, which ranges from nearly 0 to 31 mmol/L. This pattern was due to multiple reasons, which are elaborated below.

The main driver for the diverse DOC concentrations was the different irrigation rates that varied from 50 to 150 mL/day. The wheat straw mass was always set to 10 g in the microcosms. Thus, the more water is flushed through the microcosms, the higher the dilution of produced DOC in the leachate water containers. Only wheat straw mixed with rock powder microcosms were selected for Fig. 8 to eliminate the variability caused by different organic matter sources. The dilution effect for the water samples is displayed in Fig. 8, indicated by the dashed line. The path follows a constant DOC amount of 30 mmol, which was chosen arbitrarily to illustrate the pattern. For more diagrams illustrating the impact of irrigation rates on the dilution of DOC, see Supplementary Figure 4 and Fig. 5

When examining microcosms containing wheat straw and a constant irrigation rate category alone, a significant spread in leached DOC is still evident (see Fig. 8). This spread is a result of the diverse composition of the microcosms. They contain different rock types in various grain sizes and combinations of biota additions, including fungi, bacteria, and earthworms. Of the 296 microcosms containing wheat straw, the biota composition is shown in Table 5.

All those components supply DOC in varying amounts. For the experiment microorganisms were grown in a DOC-rich nutrient medium. This nutrient medium was added together with the microorganisms and can also contribute to the DOC itself. Furthermore, different microorganisms were added to the microcosms. The different species could not reveal a strong impact on the $TA_{measured}$ and other weathering indicators, but they were all grown in different nutrient media optimized for the given bacteria or fungi species to grow. Those different nutrient media can also impact the DOC concentrations.

Additionally, the different rock types and grain sizes impact the size of the pH, thereby affecting the release of DOC (Evans et al., 2005; Kalbitz et al., 2000). Generally, the highest $TA_{measured}$ and thus also pH was usually reached with microcosms containing dunite rock powder.

3.6. Comparison with other water samples from EW experiments and natural environments

To assess whether similarly high DOC concentrations occur in other EW experiments and how they impact the measured TA, the same calculations for A_C were applied to additional datasets of various environments (Table 6).

In Fig. 9, water samples from 4 different soil leaching experiments are shown, as well as water samples from the Elbe estuary region for a general DOC level comparison. A key factor is the time dependency in

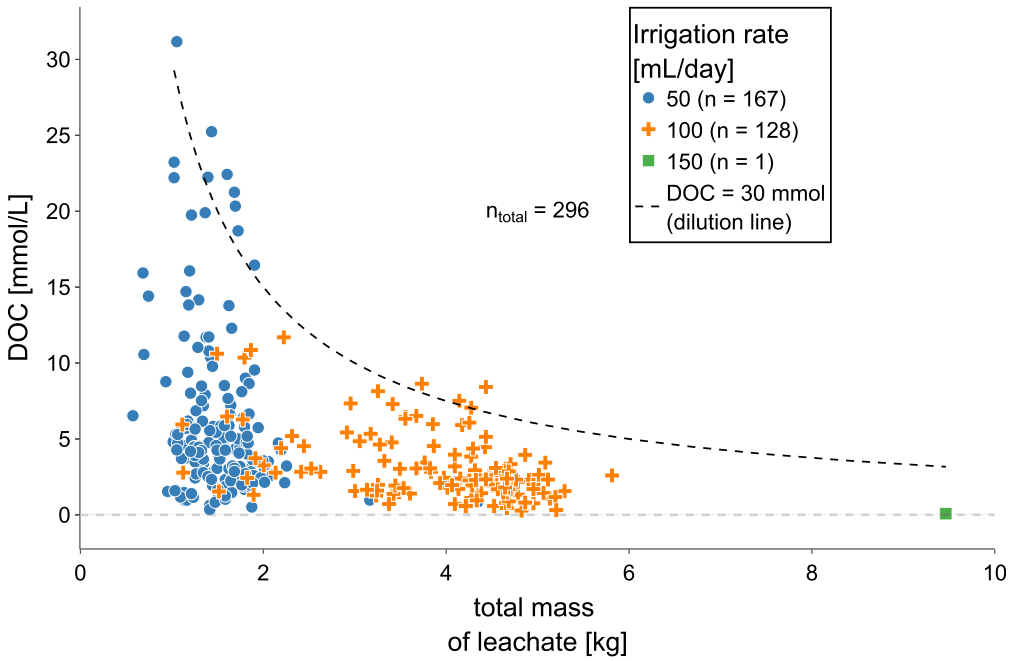

Fig. 8. Relationship between dissolved organic carbon (DOC) concentration and the total mass of leachate for microcosms containing straw. The colors represent different irrigation rates used in the microcosms. The dashed line represents a theoretical dilution line for a constant dissolved organic carbon (DOC) concentration of 30 mmol/L. (For interpretation of the references to color in this figure legend, the reader is referred to the Web version of this article.)

Table 5
Number of different microcosm categories containing rock powder and wheat straw.

Category	Count
rock powder + organic matter + bacteria + fungi	130
rock powder + organic matter + earthworms	86
rock powder + organic matter + bacteria + fungi + earthworms	58
rock powder + organic matter	22
Total	296

Table 6
Datasets used for comparison.

Dataset number	Short description
[1]	Leachate water samples from an organic-rich soil column EW experiment, excluding plants (setup in Supplementary Section 6).
[2]	Leachate water samples from a brown earth soil column EW experiment, excluding plants (setup in Supplementary Section 7).
[3]	Leachate water samples from mesocosms filled with brown earth soil comparable with [2] from an EW experiment inside a greenhouse, including grass plants from the Carbon Drawdown Initiative (Paessler et al., 2024).
[4]	Leachate water samples from a natural salt marsh soil column experiment with no rock addition (Tutiyasarn, 2024).
[5]	Water samples from the Elbe estuary along the salinity gradient, including samples with high organic mineralization rates due to prolonged residence time (Amann, 2013).
[6]	Water samples from creek outlets besides the Elbe estuary, draining organic-rich tidal marsh land soils, partly affected by sediment deposition with carbonate content (Weiss, 2013).

DOC concentrations. For the datasets [1] and [2] (Fig. 9), initially high DOC concentrations are leached from the soil, and after around 400 days, the DOC levels remain constant at a low level. In the dataset [3], one cannot see any temporal trend in DOC concentration. We attribute this to the late sampling start, such that the major DOC loss had already occurred. In dataset [4], no temporal trend in DOC concentrations was observed.

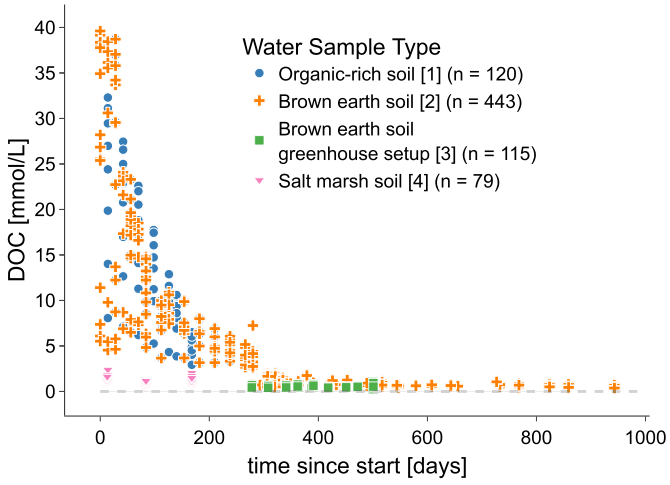

Fig. 9. DOC time series for different EW soil column experiments.

The DOC concentration in leachate water strongly depends on the experimental setup used. For datasets [1], [2], and [3], the soil was dried, homogenized, and mixed with rock powder at different application rates. Drying and rewetting the soils can lead to intense DOC leaching and can significantly increase soil organic carbon (SOC) decomposition rates (Dong et al., 2021), an effect known as the birch effect (Birch, 1958). Mechanically homogenizing the soils may have further increased SOC decomposition rates by breaking some soil aggregates. Another factor controlling DOC release is soil pH, which can increase the DOC leaching in two different ways. First, the increase in pH can enhance the solubilization of organic matter through the deprotonation of functional groups (Schnitzer, 1982). Second there is the indirect microbial effects on the organic matter solubilization also known as the pH priming effect (Andersson et al., 2000; Andersson and Nilsson, 2001; Grybos et al., 2009; Wang and Kuzyakov, 2024). The increase in the soil pH causes a priming effect of microbial activity, which mineralizes SOC (Grover et al., 2021). This mineralization leads to a release of

CO_2 and DOC. For datasets [1], [2], and [3], the soils were amended with rock powder; however, dataset [4] consists of leachate water samples from blank marshland soil without any rock powder addition.

After an initial phase of high leaching, the DOC concentrations in soil EW experiments are expected to decline until stabilization after some time. How long it takes to stabilize the DOC levels is likely a function of multiple factors. First, the initial soil pH, which controls how quickly the added rock powder will dissolve and then elevate the soil pH (Dupla et al., 2025). Second, the initial SOC content and quality, which also controls how acidic the soil reacts when increasing pH (Curtin et al., 1996). Third, the total water volume that flowed through the soil, which transports the DOC out of the soil. Fourth, the alkalinity released to the soil by the used rock powder or alkaline material, where more alkaline materials will cause a bigger soil pH increase and thereby more DOC release.

The A_C was calculated for mesocosm experiments in the greenhouse [3] and for the Elbe estuary [5], covering different zones (Amann et al., 2015) from the freshwater river part, to the organic matter decomposition zones, the oxygen minimum zone, to the outlet, as well as for tidal creeks draining organic-rich marshland soil [6]. From each dataset only a subset of the water samples was tested for $TA_{measured}$, pH, T, DIC, this led to fewer samples compared to Figs. 9 and 10. On those subsets the A_C was calculated and plotted against $TA_{measured}$ (Fig. 11). The A_C matches well with the $TA_{measured}$. This can be explained by their relatively low DOC concentrations compared to the early period of the soil column experiments (first 300 days). As a result, the calculated A_{NC} is small (Fig. 12). Only for the water samples coming from the organic-rich tidal soils, there might be some impact of A_{NC} with large uncertainty reflected by the patterns in the A_C and $TA_{measured}$ space (Fig. 12). However, the tested samples from all three datasets in Fig. 12 have no clear relationship with DOC concentration. The A_{NC} is mostly dispersed around 0 meq/kgw with just a slight positive trend.

Based on this, it can be concluded that most EW soil column experiments might exhibit an initial DOC leaching phase characterized by high DOC concentrations (Fig. 9). During this phase, the A_{NC} can likely not be neglected, and organic alkalinity may play a role in influencing the $TA_{measured}$. With lower DOC concentrations, the impact of organic alkalinity will also decline. After this initial leaching phase, the A_C will be close to the $TA_{measured}$.

From Fig. 12 one can infer that other non-organic species likely contributed to the A_{NC}. The water samples from the Elbe estuary region (datasets [3] and [6]) might have more dominant contributions from other inorganic proton acceptors (Wolf-Gladrow et al., 2007). This leads to a weak correlation of A_{NC} with the DOC concentration (Fig. 12). Only in the microcosm experiment where the organic contributions to A_{NC} outweigh other inorganic proton acceptors the DOC will correlate well with the A_{NC} (Fig. 4).

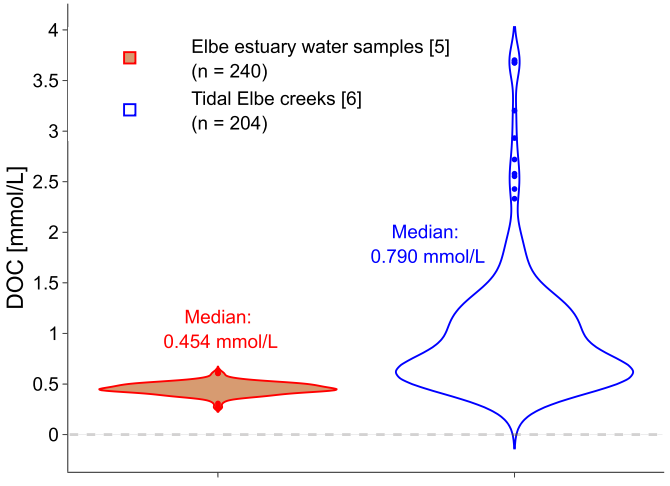

Fig. 10. DOC concentrations in Elbe estuary water samples, used as a natural baseline for a comparison for the experimental data.

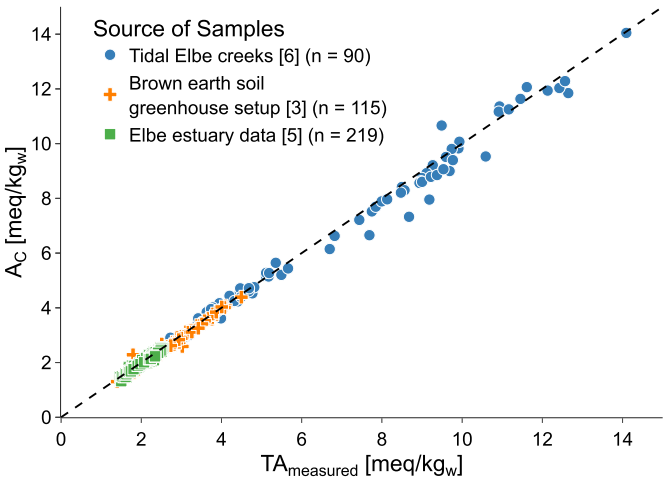

Fig. 11. Carbonate alkalinity (A_C) versus measured TA for different datasets. The dashed line represents the 1:1 line.

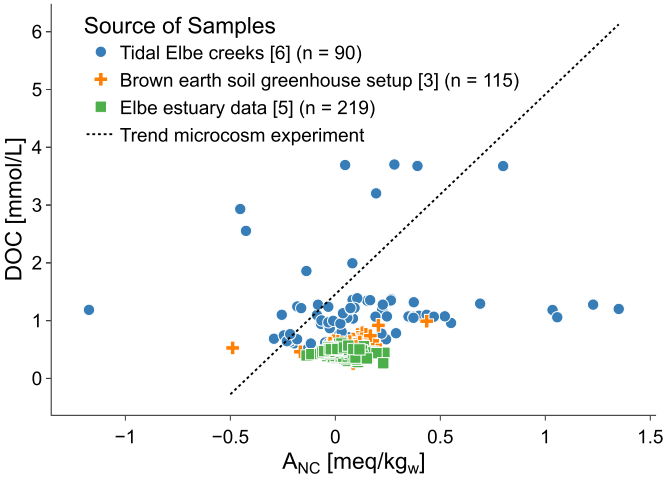

Fig. 12. DOC versus non-carbonate alkalinity (A_{NC}) for different datasets. The dashed line shows the DOC A_{NC} relationship from the microcosm leachate water samples.

Overall, the contribution of A_{NC} decreases from the microcosm leachate water scale to the mesocosms and drainage creeks from marshland soils to the Elbe estuary area (Fig. 13). While the decomposition of fresh organic matter in the microcosms provided high DOC concentrations that elevated the A_{NC} contribution, it is decreasing on larger scales. In the soil mesocosm data, the impact of DOC on A_{NC} will also be different as the available organic carbon pool is qualitatively distinct (Ukalska-Jaruga et al., 2021). In contrast to fresh organic inputs such as wheat straw, the stabilized soil organic carbon pool consists of decomposed and microbially processed material that is more resistant to further degradation. However, to analyze this quality of leached DOC in depth, samples from the initial 300 days (see Fig. 9) with high DOC concentrations would be beneficial.

Overall, in the tested microcosm leachate waters, the median A_{NC} contribution was around 5 %, while in the Elbe estuary, it is just around 1 % (Fig. 13). The water in the basin is more diluted and mineralization of DOC already occurred on the way which will convert the organic acid anions contribution to A_{NC} into A_C. The water in the basin is more diluted, and mineralization of dissolved organic carbon (DOC) has already occurred along its flow path, progressively converting the

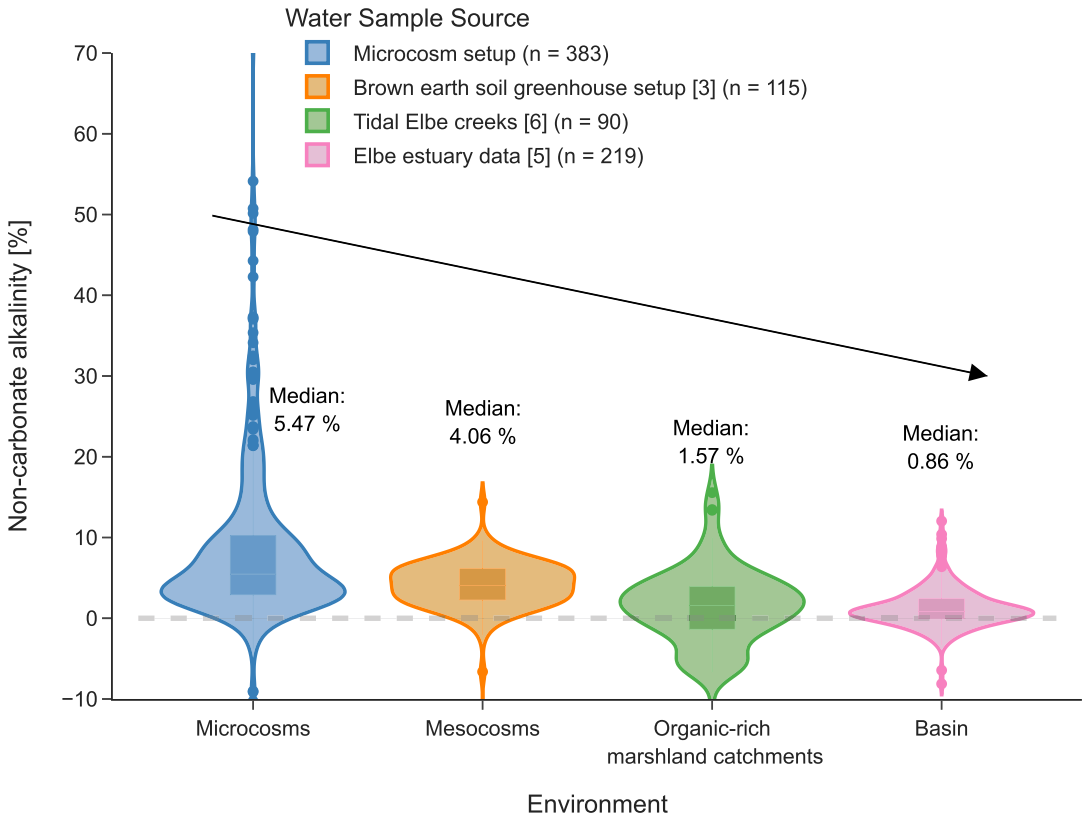

Fig. 13. Relative non-carbonate alkalinity contribution ($A_{NC}/TA_{measured}$). From left to the microcosm scale down to the Elbe River basin.

organic acid anions that contribute to A_{NC} into A_C (Hu, 2020; Xinping Hu, 2020), as it is exposed to a range of biogeochemical processes from soils to the estuarine region.

4. Conclusion

In our tested leachate water samples of a rock weathering microcosm experiment with artificial organo-mineral mixtures, the relationship between dissolved organic carbon (DOC) and non-carbonate alkalinity (A_{NC}) was quantified as $DOC = 3.461 \cdot A_{NC} + 1.462$. This indicates that approximately 3.5 DOC equivalents contribute to one total alkalinity (TA) equivalent. The relatively low factor of 3.5 suggests that not much long-chained organic acids were present, but rather the conjugate base anions of low-molecular-weight organic acids (LMWOAs). This was also verified by the abundance of acetate in DOC-rich samples. In addition, increasing DOC levels also amplified the charge balance error, as accurate TA measurements require titration to a pH below the point where organic conjugate base anions are fully protonated. In this experimental design, the initial goal was to increase carbonate alkalinity; thus, a titration with endpoints [4.5; 4.3; 4.0; 3.7] was used. In this range the observed acetate was not fully protonated. This suggests that the endpoint for titration should be adjusted to a value lower than in the definition of TA commonly used (Wolf-Gladrow et al., 2007), ensuring proper measurement for organic-rich water samples.

Organic alkalinity, comprising the conjugate base anions of organic acids, has an uncertain long-term fate. It is expected to eventually convert into CO_2 and carbonate alkalinity by anerobic pathways and photodegradation (Song et al., 2020) while maintaining charge balance of the water. A critical question for future CDR assessments using EW is determining how much additional DOC and its quality is mobilized by alkaline material application compared to its stability without EW interventions.

The organic alkalinity can be a non-neglectable part of the measured alkalinity depending on the environmental conditions and the composition of the organo-mineral substrate. In this experimental setup, organic acids were produced by decomposition of wheat straw. From the tested LMWOAs, only acetate was detected. The acetate anions could not explain all the detected non-carbonate alkalinity, but there are far more organic acids that can have an impact than the tested oxalate, citrate, and acetate. All dissolved organic matter with charged functional groups will impact the measured alkalinity.

This study demonstrates that organic alkalinity can contribute substantially to total alkalinity in short-term experiments involving fresh organic inputs, such as cropland soil incubations or artificial systems enriched with easily degradable organic matter. However, its influence diminishes over time: in long-term cropland experiments, the contribution of non-carbonate alkalinity typically falls below 5 %. This suggests that organic alkalinity is most relevant under conditions where fresh, readily deprotonatable organic compounds are actively produced or added. In soils, where most organic matter is older and more resistant to degradation, its contribution likely becomes negligible once pH stabilizes following rock powder application. Nevertheless, in cropland soil settings, it remains essential to consider this initial phase and account for the SOC loss when assessing the overall CO_2 budget. It is suggested that this aspect should be considered in publicly available databases aggregating knowledge from experiments like those conducted here, to provide a knowledge database for MRV-protocols. With this it could be possible to identify conditions where the aspect of organic alkalinity should be addressed in MRV-schemes.

CRediT authorship contribution statement

Lukas Rieder: Writing – original draft, Visualization, Validation, Software, Methodology, Investigation, Formal analysis, Data curation, Conceptualization. **Mathilde Hagens:** Writing – review & editing, Supervision, Funding acquisition. **Reinaldy Poetra:** Writing – review &

editing, Methodology, Investigation, Data curation. **Alix Vidal:** Writing – review & editing. **Tullia Calogiuri:** Writing – review & editing, Investigation, Data curation. **Anna Neubeck:** Writing – review & editing, Funding acquisition. **Abhijeet Singh:** Writing – review & editing, Investigation, Data curation. **Thomas Corbett:** Investigation, Data curation. **Harun Niron:** Investigation, Data curation. **Sara Vicca:** Writing – review & editing, Project administration, Funding acquisition. **Siegfried E. Vlaeminck:** Writing – review & editing, Funding acquisition. **Iris Janssens:** Writing – review & editing, Software, Data curation. **Tim Verdonck:** Funding acquisition, Data curation. **Ivan Janssens:** Writing – review & editing, Funding acquisition. **Xuming Li:** Investigation, Data curation. **Jens S. Hammes:** Writing – review & editing, Investigation, Data curation. **Jens Hartmann:** Writing – review & editing, Supervision, Funding acquisition, Conceptualization.

Declaration of Generative AI and AI-assisted technologies in the writing process

During the preparation of this work the authors used ChatGPT with GPT-3.5 (gpt-3.5-turbo) by OpenAI to improve the readability. After using this tool/service, the authors reviewed and edited the content as needed and take full responsibility for the content of the publication.

Funding source

The authors declare that financial support was received for the research, authorship, and/or publication of this article. The authors acknowledge funding from the European Union Horizon 2020 framework program for research and innovation (Grant agreement ID: 964545), from the Carbon Drawdown Initiative Carbdown GmbH, and by the Deutsche Forschungsgemeinschaft (DFG, German Research Foundation) under Germany's Excellence Strategy—EXC 2037 CLICCS—Climate, Climatic Change, and Society—Project Number: 390683824, contribution to the Center for Earth System Research and Sustainability (CEN) of Universität Hamburg.

Declaration of competing interest

The authors declare that they have no known competing financial interests or personal relationships that could have appeared to influence the work reported in this paper.

Acknowledgments

We acknowledge Peggy Bartsch, Harm Gooren, Joost Hooghiemstra, Tom Jäppinen, Peter Nobels, Brent Rotgans, Tamas Salanki, and Gerlinde Vink, for the support provided in the lab, and for the analyses of the samples. We also thank Ángel Velasco Sanchez, Steven Heesterman, Xuming Li, François Priels, Karen Morán Rivera, Jonna van den Berg and Kangying Xie for the help provided during the sampling. Finally, we thank the staff of Unifarm, for the provision and maintenance of the climate chamber during the experimental period.

Appendix A. Supplementary data

Supplementary data to this article can be found online at https://doi.org/10.1016/j.apgeochem.2026.106685.

Data availability

The dataset generated and analyzed during the current study has been deposited in the open-access data repository PANGAEA (https://doi.org/10.1594/PANGAEA.984825).

References

Adeleke, R., Nwangburuka, C., Oboirien, B., 2017. Origins, roles and fate of organic acids in soils: a review. South Afr. J. Bot., Le 108, 393–406. https://doi.org/10.1016/j.sajb.2016.09.002.

Amann, T., 2013. Spatio-Temporal Variability of Carbon and Silica Fluxes Through the Inner Elbe Estuary. Germany. University of Hamburg, Hamburg.

Amann, T., Weiss, A., Hartmann, J., 2015. Inorganic carbon fluxes in the inner elbe Estuary, Germany. Estuaries Coasts 38, 192–210. https://doi.org/10.1007/s12237-014-9785-6.

Andersson, S., Nilsson, S.I., 2001. Influence of pH and temperature on microbial activity, substrate availability of soil-solution bacteria and leaching of dissolved organic carbon in a mor humus. Soil Biol. Biochem. 33, 1181–1191. https://doi.org/10.1016/S0038-0717(01)00022-0.

Andersson, S., Nilsson, S.I., Saetre, P., 2000. Leaching of dissolved organic carbon (DOC) and dissolved organic nitrogen (DON) in mor humus as affected by temperature and pH. Soil Biol. Biochem. 32, 1–10. https://doi.org/10.1016/S0038-0717(99)00103-0.

Beerling, D.J., Kantzas, E.P., Lomas, M.R., Wade, P., Eufrasio, R.M., Renforth, P., Sarkar, B., Andrews, M.G., James, R.H., Pearce, C.R., Mercure, J.-F., Pollitt, H., Holden, P.B., Edwards, N.R., Khanna, M., Koh, L., Quegan, S., Pidgeon, N.F., Janssens, I.A., Hansen, J., Banwart, S.A., 2020. Potential for large-scale CO2 removal via enhanced rock weathering with croplands. Nature 583, 242–248. https://doi.org/10.1038/s41586-020-2448-9.

Berner, R.A., 2003. The long-term carbon cycle, fossil fuels and atmospheric composition. Nature 426, 323–326. https://doi.org/10.1038/nature02131.

Birch, H.F., 1958. The effect of soil drying on humus decomposition and nitrogen availability. Plant Soil 10, 9–31. https://doi.org/10.1007/BF01343734.

Bouché, M., 1977. Strategies lombriciennes. Ecol. Bull. 122–132.

Boyer, T.H., Singer, P.C., Aiken, G.R., 2008. Removal of dissolved organic matter by anion exchange: effect of dissolved organic matter properties. Environ. Sci. Technol. 42, 7431–7437. https://doi.org/10.1021/es800714d.

Breitenbach, R., Gerrits, R., Dementyeva, P., Knabe, N., Schumacher, J., Feldmann, I., Radnik, J., Ryo, M., Gorbushina, A.A., 2022. The role of extracellular polymeric substances of fungal biofilms in mineral attachment and weathering. npj Mater. Degrad. 6, 42. https://doi.org/10.1038/s41529-022-00253-1.

Bryce, C.C., Le Bihan, T., Martin, S.F., Harrison, J.P., Bush, T., Spears, B., Moore, A., Leys, N., Byloos, B., Cockell, C.S., 2016. Rock geochemistry induces stress and starvation responses in the bacterial proteome. Environ. Microbiol. 18, 1110–1121. https://doi.org/10.1111/1462-2920.13093.

Byloos, B., Maan, H., Van Houdt, R., Boon, N., Leys, N., 2018. The ability of basalt to leach nutrients and support growth of *Cupriavidus metallidurans* CH34 depends on basalt composition and element release. Geomicrobiol. J. 35, 438–446. https://doi.org/10.1080/01490451.2017.1392650.

Cai, W.-J., Wang, Y., Hodson, R.E., 1998. Acid-base properties of dissolved organic matter in the estuarine waters of Georgia, USA. Geochem. Cosmochim. Acta 62, 473–483. https://doi.org/10.1016/S0016-7037(97)00363-3.

Calogiuri, T., Hagens, M., Van Groenigen, J.W., Corbett, T., Hartmann, J., Hendriksen, R., Janssens, I., Janssens, I.A., Ledesma Dominguez, G., Loescher, G., Mortier, S., Neubeck, A., Niron, H., Poetra, R.P., Rieder, L., Struyf, E., Van Tendeloo, M., De Schepper, T., Verdonck, T., Vlaeminck, S.E., Vicca, S., Vidal, A., 2023. Design and construction of an experimental setup to enhance mineral weathering through the activity of soil organisms. J. Vis. Exp. 65563. https://doi.org/10.3791/65563.

Calogiuri, T., Janssens, I., Vidal, A., Van Groenigen, J.W., Verdonck, T., Corbett, T., Hartmann, J., Neubeck, A., Niron, H., Poetra, R.P., Rieder, L., Servotte, T., Singh, A., Van Tendeloo, M., Vlaeminck, S.E., Vicca, S., Hagens, M., 2024. Earthworms foster carbon capture during mineral weathering both alive and after dying through contrasting pathways. Submitt. Appl. Geochem.

Curtin, D., Campbell, C., Messer, D., 1996. Prediction of Titratable Acidity and Soil Sensitivity to Ph Change. Wiley Online Library.

de los Ríos, A., Souza-Egipsy, V., 2021. 1.1 the interface of rocks and microorganisms. Life Rock Surf 3–38.

Dickson, A.G., Sabine, C.L., Christian, J.R., Bargeron, C.P., 2007. North Pacific marine science organization. Guide to Best Practices for Ocean CO2 Measurements. PICES special publication. North Pacific Marine Science Organization, Sidney, BC.

DIN 38402-62, 2014. DIN 38402-62:2014-12, Deutsche Einheitsverfahren zur Wasser-, Abwasser- und Schlammuntersuchung_- Allgemeine Angaben (Gruppe_A)_- Teil_62: Plausibilitätskontrolle von Analysendaten durch Ionenbilanzierung_(A_62). https://doi.org/10.31030/2248076.

DIN EN 27888:1993-11, Wasserbeschaffenheit; Bestimmung Der Elektrischen Leitfähigkeit (ISO_7888:1985); Deutsche Fassung EN_27888:1993, 1993. . Beuth Verlag GmbH. https://doi.org/10.31030/2569904.

Dong, H., Zhang, S., Lin, J., Zhu, B., 2021. Responses of soil microbial biomass carbon and dissolved organic carbon to drying-rewetting cycles: a meta-analysis. Catena 207, 105610. https://doi.org/10.1016/j.catena.2021.105610.

Drever, J.I., Stillings, L.L., 1997. The role of organic acids in mineral weathering. Colloids Surf. A Physicochem. Eng. Asp. 120, 167–181. https://doi.org/10.1016/S0927-7757(96)03720-X.

Dupla, X., Brantley, S.L., Paulo, C., Möller, B., Power, I.M., Grand, S., 2025. Geochemical drivers of enhanced rock weathering in soils. In: Beech, M. (Ed.), Geoengineering and Climate Change. Wiley, pp. 207–230. https://doi.org/10.1002/9781394204847.ch13.

Evans, C.D., Monteith, D.T., Cooper, D.M., 2005. Long-term increases in surface water dissolved organic carbon: observations, possible causes and environmental impacts. Environ. Pollut. 137, 55–71. https://doi.org/10.1016/j.envpol.2004.12.031.

Fritz, S.J., 1994. A survey of charge-balance errors on published analyses of potable ground and surface waters. Groundwater 32, 539–546. https://doi.org/10.1111/j.1745-6584.1994.tb00888.x.
Georgiadis, A., Marhan, S., Lattacher, A., Mäder, P., Rennert, T., 2019. Do earthworms affect the fractionation of silicon in soil? Pedobiologia 75, 1–7. https://doi.org/10.1016/j.pedobi.2019.05.001.
Gerrits, R., Pokharel, R., Breitenbach, R., Radnik, J., Feldmann, I., Schuessler, J.A., Von Blanckenburg, F., Gorbushina, A.A., Schott, J., 2020. How the rock-inhabiting fungus K. Petricola A95 enhances olivine dissolution through attachment. Geochem. Cosmochim. Acta 282, 76–97. https://doi.org/10.1016/j.gca.2020.05.010.
Goll, D., Ciais, P., Amann, T., Buermann, W., Chang, J., Eker, S., Hartmann, J., Janssens, I., Li, W., Obersteiner, M., Penuelas, J., Tanaka, K., Vicca, S., 2021. Potential CO2 removal from enhanced weathering by ecosystem responses to powdered rock. Nat. Geosci. 14, 1–5. https://doi.org/10.1038/s41561-021-00798-x.
Grover, S.P., Butterly, C.R., Wang, X., Gleeson, D.B., Macdonald, L.M., Tang, C., 2021. Liming and priming: the long-term impact of pH amelioration on mineralisation may negate carbon sequestration gains. Soil Secur. 3, 100007. https://doi.org/10.1016/j.soisec.2021.100007.
Grybos, M., Davranche, M., Gruau, G., Petitjean, P., Pédrot, M., 2009. Increasing pH drives organic matter solubilization from wetland soils under reducing conditions. Geoderma 154, 13–19. https://doi.org/10.1016/j.geoderma.2009.09.001.
Hammer, K., Schneider, B., Kuliński, K., Schulz-Bull, D.E., 2017. Acid-base properties of Baltic Sea dissolved organic matter. J. Mar. Syst. 173, 114–121. https://doi.org/10.1016/j.jmarsys.2017.04.007.
Hansen, H.P., Koroleff, F., 1999. Determination of nutrients. In: Grasshoff, K., Kremling, K., Ehrhardt, M. (Eds.), Methods of Seawater Analysis. Wiley, pp. 159–228. https://doi.org/10.1002/9783527613984.ch10.
Harned, H.S., Davis Jr, R., 1943. The ionization constant of carbonic acid in water and the solubility of carbon dioxide in water and aqueous salt solutions from 0 to 50. J. Am. Chem. Soc. 65, 2030–2037.
Hartmann, J., West, A.J., Renforth, P., Köhler, P., De La Rocha, C.L., Wolf-Gladrow, D.A., Dürr, H.H., Scheffran, J., 2013. Enhanced chemical weathering as a geoengineering strategy to reduce atmospheric carbon dioxide, supply nutrients, and mitigate ocean acidification. Rev. Geophys. 51, 113–149. https://doi.org/10.1002/rog.20004.
Hastings, A.B., Sendroy Jr, J., 1925. The effect of variation in ionic strength on the apparent first and second dissociation constants of carbonic acid. J. Biol. Chem. 65, 445–455.
Heinsbroek, A., 2021. Phreeqpython: Vitens Viphreeqc Wrapper and Utilities.
Herdtweck, E., Kornprobst, T., Sieber, R., Straver, L., Plank, J., 2011. Crystal Structure, Synthesis, and Properties of *tri* -Calcium *di* -Citrate *tetra* -Hydrate [Ca_3 (C_6 H_5 O_7)$_2$ (H_2 O)$_2$]·2H_2 O. Z. Für Anorg. Allg. Chem. 637, 655–659. https://doi.org/10.1002/zaac.201100088.
Hu, X., 2020. Effect of organic alkalinity on seawater buffer capacity: a numerical exploration. Aquat. Geochem. 26, 161–178. https://doi.org/10.1007/s10498-020-09375-x.
Hu, Xinping, 2020. The curious role of organic alkalinity in seawater carbonate chemistry. Ocean Carbon Biogeochem. URL. https://www.us-ocb.org/the-curious-role-of-organic-alkalinity-in-seawater-carbonate-chemistry/. accessed 5.9.25.
Hunt, C.W., Salisbury, J.E., Vandemark, D., 2011. Contribution of non-carbonate anions to total alkalinity and overestimation of *p* CO_2 in New England and New Brunswick rivers. Biogeosciences 8, 3069–3076. https://doi.org/10.5194/bg-8-3069-2011.
IPCC, 2022a. IPCC AR6 WGIII: CDR factsheet [WWW Document]. URL. https://www.ipcc.ch/report/ar6/wg3/downloads/outreach/IPCC_AR6_WGIII_Factsheet_CDR.pdf. accessed 7.12.24.
IPCC, 2022b. Climate Change 2022 - Mitigation of Climate Change: Working Group III Contribution to the Sixth Assessment Report of the Intergovernmental Panel on Climate Change, first ed. Cambridge University Press. https://doi.org/10.1017/9781009157926.
Kalbitz, K., Solinger, S., Park, J.-H., Michalzik, B., Matzner, E., 2000. Controls on the dynamics of dissolved organic matter in soils: a review. Soil Sci. 165, 277.
Karki, R., Chuenchart, W., Surendra, K.C., Shrestha, S., Raskin, L., Sung, S., Hashimoto, A., Kumar Khanal, S., 2021. Anaerobic co-digestion: current status and perspectives. Bioresour. Technol. 330, 125001. https://doi.org/10.1016/j.biortech.2021.125001.
Kerr, D.E., Brown, P.J., Grey, A., Kelleher, B.P., 2021. The influence of organic alkalinity on the carbonate system in coastal waters. Mar. Chem. 237, 104050. https://doi.org/10.1016/j.marchem.2021.104050.
Kim, H., Lee, K., 2009. Significant contribution of dissolved organic matter to seawater alkalinity. Geophys. Res. Lett. 36. https://doi.org/10.1029/2009GL040271, 2009GL040271.
Ko, Y.H., Lee, K., Eom, K.H., Han, I., 2016. Organic alkalinity produced by phytoplankton and its effect on the computation of ocean carbon parameters. Limnol. Oceanogr. 61, 1462–1471. https://doi.org/10.1002/lno.10309.
Koenig, N., 2005. Handbuch Forstliche Analytik - Eine Loseblatt-Sammlung Der Analysemethoden Im Forstbereich.
Kuliński, K., Schneider, B., Hammer, K., Machulik, U., Schulz-Bull, D., 2014. The influence of dissolved organic matter on the acid–base system of the Baltic Sea. J. Mar. Syst. 132, 106–115. https://doi.org/10.1016/j.jmarsys.2014.01.011.
Küsel, K., Drake, H.L., 1998. Microbial turnover of low molecular weight organic acids during leaf litter decomposition. Soil Biol. Biochem. 31, 107–118. https://doi.org/10.1016/S0038-0717(98)00111-4.
Kutus, B., Gaona, X., Pallagi, A., Pálinkó, I., Altmaier, M., Sipos, P., 2020. Recent advances in the aqueous chemistry of the calcium(II)-gluconate system – Equilibria, structure and composition of the complexes forming in neutral and in alkaline solutions. Coord. Chem. Rev. 417, 213337. https://doi.org/10.1016/j.ccr.2020.213337.
Lasaga, A.C., Soler, J.M., Ganor, J., Burch, T.E., Nagy, K.L., 1994. Chemical weathering rate laws and global geochemical cycles. Geochem. Cosmochim. Acta 58, 2361–2386. https://doi.org/10.1016/0016-7037(94)90016-7.
Lazo, D.E., Dyer, L.G., Alorro, R.D., 2017. Silicate, phosphate and carbonate mineral dissolution behaviour in the presence of organic acids: a review. Miner. Eng. 100, 115–123. https://doi.org/10.1016/j.mineng.2016.10.013.
Lee, C.-H., Lee, K., Lee, J.-S., Jeong, K.-Y., Ko, Y.-H., 2024. Persistent organic alkalinity in the ocean. Geochem. Cosmochim. Acta 387, 53–62. https://doi.org/10.1016/j.gca.2024.06.010.
Physical constants of inorganic compounds (continued). In: Lide, David R. (Ed.), 2005. CRC Handbook of Chemistry and Physics. CRC Press, Taylor & Francis Group, Boca Raton, FL.
Liu, S., Butman, D.E., Raymond, P.A., 2020. Evaluating CO2 calculation error from organic alkalinity and pH measurement error in low ionic strength freshwaters. Limnol Oceanogr. Methods 18, 606–622. https://doi.org/10.1002/lom3.10388.
Liu, H., Liu, X., Li, X., Fu, Z., Lian, B., 2021. The molecular regulatory mechanisms of the bacteria involved in serpentine weathering coupled with carbonation. Chem. Geol. 565, 120069. https://doi.org/10.1016/j.chemgeo.2021.120069.
Lozovik, P.A., 2005. Contribution of organic acid anions to the alkalinity of natural humic water. J. Anal. Chem. 60, 1000–1004. https://doi.org/10.1007/s10809-005-0226-3.
Lubbers, I.M., Van Groenigen, K.J., Fonte, S.J., Six, J., Brussaard, L., Van Groenigen, J. W., 2013. Greenhouse-gas emissions from soils increased by earthworms. Nat. Clim. Change 3, 187–194. https://doi.org/10.1038/nclimate1692.
Lukawska-Matuszewska, K., 2016. Contribution of non-carbonate inorganic and organic alkalinity to total measured alkalinity in pore waters in marine sediments (Gulf of Gdansk, S-E Baltic Sea). Mar. Chem. 186, 211–220. https://doi.org/10.1016/j.marchem.2016.10.002.
Lukawska-Matuszewska, K., Grzybowski, W., Szewczun, A., Tarasiewicz, P., 2018. Constituents of organic alkalinity in pore water of marine sediments. Mar. Chem. 200, 22–32. https://doi.org/10.1016/j.marchem.2018.01.012.
Lv, X., Hao, J., Zhao, Y., Li, C., Quan, W., 2023. Seasonal variations of low-molecular-weight organic acids in three evergreen broadleaf rhododendron forests. Metabolites 13, 119. https://doi.org/10.3390/metabo13010119.
Middelburg, J.J., Soetaert, K., Hagens, M., 2020. Ocean alkalinity, buffering and biogeochemical processes. Rev. Geophys. 58. https://doi.org/10.1029/2019RG000681 e2019RG000681.
Miessler, G.L., Fischer, P.J., Tarr, D.A., 2014. Inorganic Chemistry, fifth ed. Pearson, Boston.
Mostofa, K.M.G., Liu, C., Mottaleb, M.A., Wan, G., Ogawa, H., Vione, D., Yoshioka, T., Wu, F., 2013. Dissolved organic matter in natural waters. In: Mostofa, K.M.G., Yoshioka, T., Mottaleb, A., Vione, D. (Eds.), Photobiogeochemistry of Organic Matter. Environmental Science and Engineering. Springer Berlin Heidelberg, Berlin, Heidelberg, pp. 1–137. https://doi.org/10.1007/978-3-642-32223-5_1.
Muller, F.L.L., Bleie, B., 2008. Estimating the organic acid contribution to coastal seawater alkalinity by potentiometric titrations in a closed cell. Anal. Chim. Acta 619, 183–191. https://doi.org/10.1016/j.aca.2008.05.018.
Müller, H., Bourcet, L., Hanfland, M., 2021. Iron(II)oxalate dihydrate—humboldtine: synthesis, spectroscopic and structural properties of a versatile precursor for high pressure research. Minerals 11, 113. https://doi.org/10.3390/min11020113.
Neaman, A., 2005. Implications of the evolution of organic acid moieties for basalt weathering over geological time. Am. J. Sci. 305, 147–185. https://doi.org/10.2475/ajs.305.2.147.
NIST46, 2013. Critically selected stability constants of metal complexes: version 8.0. https://doi.org/10.18434/M32154.
Novozamsky, I., Van Eck, R., Houba, V.J.G., Van Der Lee, J.J., 1996. Solubilization of plant tissue with nitric acid-hydrofluoric acid-hydrogen peroxide in a closed-system microwave digestor. Commun. Soil Sci. Plant Anal. 27, 867–875. https://doi.org/10.1080/00103629609369603.
Paessler, D., Steffens, R., Hammes, J., Smet, I., 2024. Insights from monitoring leachate alkalinity, pCO_2 and CO_2 efflux of 400 weathering experiments over one year. Working paper -V1.0 -April 11th 2024. https://doi.org/10.13140/RG.2.2.14022.28485.
Perminova, I.V., Frimmel, F.H., Kudryavtsev, A.V., Kulikova, N.A., Abbt-Braun, G., Hesse, S., Petrosyan, V.S., 2003. Molecular weight characteristics of humic substances from different environments as determined by size exclusion chromatography and their statistical evaluation. Environ. Sci. Technol. 37, 2477–2485. https://doi.org/10.1021/es0258069.
Pittman, E.D., Lewan, M.D., 1994. Organic Acids in Geological Processes. Springer Berlin Heidelberg, Berlin, Heidelberg.
Po, H.N., Senozan, N.M., 2001. The henderson-hasselbalch equation: its history and limitations. J. Chem. Educ. 78, 1499. https://doi.org/10.1021/ed078p1499.
Pokharel, R., Gerrits, R., Schuessler, J.A., Von Blanckenburg, F., 2019. Mechanisms of olivine dissolution by rock-inhabiting fungi explored using magnesium stable isotopes. Chem. Geol. 525, 18–27. https://doi.org/10.1016/j.chemgeo.2019.07.001.
Rensink, S., Van Nieuwenhuijzen, E.J., Sailer, M.F., Struck, C., Wösten, H.A.B., 2024. Use of aureobasidium in a sustainable economy. Appl. Microbiol. Biotechnol. 108, 202. https://doi.org/10.1007/s00253-024-13025-5.
Rodriguez-Gomez, D., Lehmann, L., Schultz-Jensen, N., Bjerre, A.B., Hobley, T.J., 2012. Examining the potential of plasma-assisted pretreated wheat straw for enzyme production by Trichoderma reesei. Appl. Biochem. Biotechnol. 166, 2051–2063. https://doi.org/10.1007/s12010-012-9631-x.
Rosenstock, N.P., Van Hees, P.A.W., Fransson, P.M.A., Finlay, R.D., Rosling, A., 2019. Biological enhancement of mineral weathering by *Pinus sylvestris* seedlings – effects of plants, ectomycorrhizal fungi, and elevated CO_2. Biogeosciences 16, 3637–3649. https://doi.org/10.5194/bg-16-3637-2019.

Schnitzer, M., 1982. Organic matter characterization. In: Page, A.L. (Ed.), Agronomy Monographs. Wiley, pp. 581–594. https://doi.org/10.2134/agronmonogr9.2.2ed.c30.
Schoeman, M.W., Dickinson, D.J., 1996. Aureobasidium pullulans can utilize simple aromatic compounds as a sole source of carbon in liquid culture. Lett. Appl. Microbiol. 22, 129–131. https://doi.org/10.1111/j.1472-765X.1996.tb01125.x.
Schuiling, R.D., Krijgsman, P., 2006. Enhanced weathering: an effective and cheap tool to sequester Co2. Clim. Change 74, 349–354. https://doi.org/10.1007/s10584-005-3485-y.
Schwartzman, D., 2015. The geobiology of weathering: a 13th hypothesis. https://doi.org/10.48550/ARXIV.1509.04234.
Schwarzenbach, R.P., Imboden, D.M., Gschwend, P.M., 2003. Environmental Organic Chemistry, second ed. Wiley, Hoboken, N.J. https://doi.org/10.1002/0471649643.
Seifritz, W., 1990. CO2 disposal by means of silicates. Nature 345, 486. https://doi.org/10.1038/345486b0, 486.
Sharp, J.D., Byrne, R.H., 2020. Interpreting measurements of total alkalinity in marine and estuarine waters in the presence of proton-binding organic matter. Deep-Sea Res. Part A Oceanogr. Res. Pap. 165, 103338. https://doi.org/10.1016/j.dsr.2020.103338.
Smith, S., Geden, O., Gidden, M., Lamb, W., Nemet, G., Minx, J., Buck, H., Burke, J., Cox, E., Edwards, M., 2024. The State of Carbon Dioxide Removal.
Solomon, T., 2001. The definition and unit of ionic strength. J. Chem. Educ. 78, 1691. https://doi.org/10.1021/ed078p1691.
Song, W., Ogawa, N., Oguchi, C.T., Hatta, T., Matsukura, Y., 2007. Effect of Bacillus subtilis on granite weathering: a laboratory experiment. Catena 70, 275–281. https://doi.org/10.1016/j.catena.2006.09.003.
Song, S., Wang, Z.A., Gonneea, M.E., Kroeger, K.D., Chu, S.N., Li, D., Liang, H., 2020. An important biogeochemical link between organic and inorganic carbon cycling: effects of organic alkalinity on carbonate chemistry in coastal waters influenced by intertidal salt marshes. Geochem. Cosmochim. Acta 275, 123–139. https://doi.org/10.1016/j.gca.2020.02.013.
Stumm, W., Morgan, J.J., 1996. Aquatic Chemistry - Chemical Equilibria and Rates in Natural Waters, third ed. John Wiley AND Sons, New York.
Suzuki, Y., Matsubara, T., Hoshino, M., 2003. Breakdown of mineral grains by earthworms and beetle larvae. Geoderma 112, 131–142. https://doi.org/10.1016/S0016-7061(02)00300-2.
Szubstarska, J., Jarzyńska, G., Falandysz, J., 2012. Trace elements in variegated bolete (Suillus variegatus) fungi. Chem. Pap. 66. https://doi.org/10.2478/s11696-012-0216-5.
Tani, M., Shida, K.S., Tsutsuki, K., Kondo, R., 2001. Determination of water-soluble low-molecular-weight organic acids in soils by ion chromatography. Soil Sci. Plant Nutr. 47, 387–397. https://doi.org/10.1080/00380768.2001.10408401.
Tutiyasarn, P., 2024. Effect of Biota on Soil Mineral Dissolution in Salt Marsh Sediment. University of Hamburg, Hamburg.
Ukalska-Jaruga, A., Bejger, R., Debaene, G., Smreczak, B., 2021. Characterization of soil organic matter individual fractions (fulvic acids, humic acids, and humins) by spectroscopic and electrochemical techniques in agricultural soils. Agronomy 11, 1067. https://doi.org/10.3390/agronomy11061067.
US EPA, O, 2013. MINTEQA2 equilibrium speciation model [WWW Document]. URL. https://www.epa.gov/hydrowq/minteqa2-equilibrium-speciation-model. accessed 11.11.24.
Van Der Sluys, W.G., 2001. The solubility rules: why are all acetates soluble? J. Chem. Educ. 78, 111. https://doi.org/10.1021/ed078p111.
Vavrusova, M., Skibsted, L.H., 2016. Aqueous solubility of calcium citrate and interconversion between the tetrahydrate and the hexahydrate as a balance between endothermic dissolution and exothermic complex formation. Int. Dairy J. 57, 20–28. https://doi.org/10.1016/j.idairyj.2016.02.033.
Vogt, R.D., Garmo, Ø.A., Austnes, K., Kaste, Ø., Haaland, S., Sample, J.E., Thrane, J.-E., Skancke, L.B., Gundersen, C.B., De Wit, H.A., 2024. Factors governing site and charge density of dissolved natural organic matter. Water 16, 1716. https://doi.org/10.3390/w16121716.
Walker, J.C., Hays, P., Kasting, J.F., 1981. A negative feedback mechanism for the long-term stabilization of Earth's surface temperature. J. Geophys. Res., Oceans 86, 9776–9782.
Wang, C., Kuzyakov, Y., 2024. Soil organic matter priming: the pH effects. Glob. Change Biol. 30, e17349. https://doi.org/10.1111/gcb.17349.
Weiss, A., 2013. The Silica and Inorganic Carbon System in Tidal Marshes of the Elbe Estuary, Germany : Fluxes and spatio-temporal Patterns. University of Hamburg, Hamburg.
Welch, S.A., Ullman, W.J., 1993. The effect of organic acids on plagioclase dissolution rates and stoichiometry. Geochem. Cosmochim. Acta 57, 2725–2736. https://doi.org/10.1016/0016-7037(93)90386-B.
Welch, S.A., Taunton, A.E., Banfield, J.F., 2002. Effect of microorganisms and microbial metabolites on apatite dissolution. Geomicrobiol. J. 19, 343–367. https://doi.org/10.1080/01490450290098414.
Wiesenbauer, J., Gorka, S., Jenab, K., Schuster, R., Kumar, N., Rottensteiner, C., König, A., Kraemer, S., Inselsbacher, E., Kaiser, C., 2025. Preferential use of organic acids over sugars by soil microbes in simulated root exudation. Soil Biol. Biochem. 203, 109738. https://doi.org/10.1016/j.soilbio.2025.109738.
Wolf-Gladrow, D.A., Zeebe, R.E., Klaas, C., Körtzinger, A., Dickson, A.G., 2007. Total alkalinity: the explicit conservative expression and its application to biogeochemical processes. Mar. Chem. 106, 287–300. https://doi.org/10.1016/j.marchem.2007.01.006.
Xiao, M., Wu, F., 2014. A review of environmental characteristics and effects of low-molecular weight organic acids in the surface ecosystem. J. Environ. Sci. 26, 935–954. https://doi.org/10.1016/S1001-0742(13)60570-7.
Yang, B., Byrne, R.H., Lindemuth, M., 2015. Contributions of organic alkalinity to total alkalinity in coastal waters: a spectrophotometric approach. Mar. Chem. 176, 199–207. https://doi.org/10.1016/j.marchem.2015.09.008.